Received: 12 January 2021 | Revised: 15 November 2021 | Accepted: 16 November 2021

DOI: 10.1002/eqe.3584

RESEARCH ARTICLE

WILEY

In-plane/out-of-plane interaction of strong masonry infills: From cyclic tests to out-of-plane verifications

Paolo Morandi[1] | **Sanja Hak**[2] | **Riccardo R. Milanesi**[3] | **Guido Magenes**[3]

[1] Eucentre, Department of Structures and Infrastructures, Pavia, Italy

[2] Department of Structural Safety, Basler & Hofmann AG, Zurich, Switzerland

[3] Deptartment of Civil Engineering and Architecture, University of Pavia, Pavia, Italy

Correspondence
Paolo Morandi, Department of Structures and Infrastructures, Eucentre, Pavia, Italy.
Email: paolo.morandi@eucentre.it

Funding information
ANDIL (Italian Association of Clay Brick and Tile Producers); Department of the Italian Civil Protection

Abstract

The construction of RC frame structures with masonry infills is part of the traditional building practice in many European countries and worldwide. Several studies have been recently conducted to improve further the understanding of the seismic response of masonry infills, which are mainly focused on weak/slender clay masonry panels representing a common typology of the past, whereas very limited research has been devoted to stronger/thicker masonry infills, which nowadays are being adopted with increasing frequency in newly designed RC structures for their excellent thermal and acoustic performance. In order to fill this gap, within a systematic experimental and numerical research program, the in-plane and out-of-plane experimental response of 'strong' masonry infills has been investigated at the Eucentre and the University of Pavia. In particular, this paper presents the framework and discusses the results of out-of-plane static cyclic tests on full-scale, single-storey, single-bay RC frame specimens infilled with 35 cm thick tongue and groove clay unit walls, the related damage propagation and the failure mechanisms. The in-plane/out-of-plane experimental interaction evaluated in terms of stiffness and strength reduction and period increase in function of previous in-plane damage is also introduced, with the aim of providing a simplified out-of-plane strength verification within the European codified design procedures.

KEYWORDS

design implications, in-plane/out-of-plane interaction, seismic strength verifications, strong clay masonry infills, out-of-plane real-scale tests

1 | INTRODUCTION

In line with the current building practice, unreinforced clay masonry infills are commonly adopted for the construction of enclosures and partitions in RC framed structures. Masonry panels are usually constructed in complete contact and after the hardening of the surrounding RC frame, without the provision of any gap or connection around the boundaries. Moreover, infills with perforated blocks and/or with lightweight material characterised by medium/large thickness (i.e., larger than 20–25 cm) are particularly appealing thanks to their acoustic and thermal properties, along with their simple and cost-effective construction process. Such types of infills are nowadays being adopted with increasing frequency in newly designed RC structures, even in earthquake prone regions, in partial substitution of masonry typologies traditionally realised with thinner single or double-leaf masonry panels (usually less than 12–15 cm thick) with highly

(A) (B)

FIGURE 1 Example of earthquake damages on infills: (A) building with modern infill typology; (B) combined in-plane and out-of-plane effects

perforated horizontally hollowed clay blocks. The former typology can be defined as robust/strong, while the latter as weak/slender.

Nevertheless, damage to masonry infills induced by earthquakes can represent threat to human lives and lead to extensive economic losses, as demonstrated by several field observations, once more in recent years, as in L'Aquila 2009 (see e.g., 1,2), in Emilia 2012 (see e.g., 3), in Central Italy (see e.g., 4), also for the case of recently constructed RC buildings (see Figure 1A). As noticed in many post-seismic inspections (see e.g., Figure 1B), the more extensive damages on infills are not located at the top storeys of infilled frames, where larger out-of-plane seismic actions are expected, but at the bottom/intermediate levels, where higher in-plane drift demands occur, proving that masonry panels decrease their out-of-plane stability when they are subjected to in-plane action. In fact, the simultaneous effects of the in-plane and out-of-plane seismic action produce a decrement of the in-plane deformation capacity due to out-of-plane action and a reduction of the out-of-plane strength due to in-plane action. Although the significance of effects arising from the interaction of in-plane and out-of-plane infill damage has been acknowledged, in relation to earthquake damage surveys (e.g., 5) as well as experimental or numerical investigations (e.g., 6), the complicated mechanism of correlation has not been sufficiently studied yet. Hence, as regards the control/limitation of interaction effects related to in-plane and out-of-plane infill damage, some essential questions remained unsolved. Also, additional improvements in currently adopted infill verification and detailing procedures appear to be necessary.

A significant number of experimental investigations related to the seismic performance of masonry infilled frames have been carried out in the past, focusing, however, mainly on the in-plane response and only on selected masonry typologies like clay bricks and concrete blocks. Fewer tests have been conducted to study the out-of-plane response and even less on the mutual in-plane/out-of-plane interaction. Within these latter, one of the first attempts to correlate the in-plane and out-of-plane response was carried out by Angel et al.,[7] where pseudo-static cyclic in-plane tests were followed by out-of-plane tests on the same specimens previously damaged in-plane. Few years later, Calvi and Bolognini[8] and, more recently, several other researchers[9–14] have performed experimental campaigns within a similar experimental framework, examining different infill typologies. The execution of in-plane/out-of-plane combined tests has been recently enhanced also for the evaluation of the seismic response of different innovative infill solutions, for example of sliding joints systems, as reported elsewhere,[15] where out-of-plane tests on a shaking table were performed following in-plane cyclic tests. Among the experimental campaigns on innovative infills, tests related to simultaneous in-plane/out-of-plane effects have also been very recently performed, for example, by Manzini et al.[16] through shaking table tests and by Butenweg et al.[17] through static cyclic tests. An updated review of experimental and analytical/numerical studies on the out-of-plane behaviour of masonry infilled frames can be found in Di Trapani et al.,[18] Anic et al.[19] and Cavaleri et al.[20]

However, limited experimental tests have been carried out on real scale infilled RC specimens and, among these, only the investigations conducted by Hak et al.[12] and da Porto et al.[9] have been devoted to the study of masonry infills with thick/strong masonry representing a modern typology in newly designed buildings, whereas the others mainly focused on weak masonry, for example, characterised by horizontally highly perforated thin clay block masonry (8–12 cm thick infills), typical of non-recent constructions.

According to the European code for seismic design of structures[21] and related national codes, for example, the Italian Norms of Construction,[22] masonry infills are thought to be verified as non-structural elements. Clearly, in the design of new buildings the limitation of infill damage is aimed to be implemented through the verification of allowable in-plane drifts and a number of specific measures. However, the practical application of existing regulations reveals significant shortcomings. Most importantly, the possible reduction of out-of-plane strength resulting from previous or simultaneous in-plane damage is not accounted for and even the evaluation of the out-of-plane resistance of undamaged infills is completely overlooked. In fact, in the European seismic codes, a clear method is only present for the evaluation of the out-of-plane seismic action on the panels, whereas, for the estimation of the out-of-plane resistance, a possibility is to adopt the criteria included in EC6 on masonry walls, anyhow specifically developed only for non-seismic actions.

Nevertheless, the importance to account for the in-plane/out-of-plane interaction was to some extent recognised through a number of investigations. Angel et al.[7] firstly proposed an expression that related the reduction of the out-of-plane strength with the in-plane drift demand in function of the slenderness of the infills. Later, Morandi et al.[23] introduced reduction coefficients based on stepwise/linear expressions describing a decrease of out-of-plane strength in function of increasing in-plane drift demand, reinterpreting the experimental outcomes by Calvi and Bolognini[8] on weak unreinforced and lightly reinforced masonry infills. From then on, other expressions for the degradation of the out-of-plane resistance and stiffness were proposed by several authors, for example, by Verlato et al.,[24] more recently, by Furtado et al.,[11,25] Akhoundi et al.,[26] Ricci et al.[14] and da Porto et al.,[27] where the formulations were calibrated according to experimental campaigns mainly conducted on weak/thin masonry infills. The verification of infills for combined in-plane and out-of-plane actions has been included in few existing recommendations for the assessment of existing buildings, for example, in FEMA 306 (1998), where the expressions based of the study by Angel et al.[7] have been included. Finally, Al-Chaar[28] firstly proposed a criterion for the reduction of the in-plane infill drift capacity as a function of the out-of-plane action/strength.

Therefore, in order to improve the understanding on the in-plane and out-of-plane seismic behaviour of modern masonry infills and of the current seismic design approach for new RC infilled structures, strong masonry infills made up by 35 cm thick tongue and groove clay units, constructed in full contact with the surrounding frame, have been investigated within the scope of a systematic research campaign. In particular, in-plane cyclic tests followed by out-of-plane cyclic tests on previously in-plane damaged specimens of full-scale, single-storey, single-bay RC frames infilled with the considered strong infill typology have been carried out at the Eucentre and the University of Pavia. Although the results of the in-plane tests have already been discussed in Morandi et al.[29] and an overview of the out-of-plane tests on previously damaged specimens has been already reported in Hak et al.,[12] in this paper the attention is focused on the interpretation of the out-of-plane tests to define possible trends of the out-of-plane stiffness, elastic period and strength in function of previously in-plane damaged panels. In order to find the initial point of such trends, an additional out-of-plane test on a specimen undamaged in-plane of the same masonry infill typology has been recently executed and the results of its lateral response have been here presented. Proposals for a simplified design approach within the European codified procedures are provided, accounting for expected levels of in-plane damage in the out-of-plane safety verification.

2 | EXPERIMENTAL CAMPAIGN

2.1 | Description of the specimens and material characterisation

The experimental campaign has included cyclic static tests on fully and partially infilled (and bare) full-scale single-storey, single-bay 4.22 × 2.95 m RC frames in both directions (in-plane and out-of-plane), as summarised in Table 1 and illustrated in Figure 2A–C. The tested frames were newly designed according to European code provisions.

All the results and the interpretation of the in-plane tests have already been discussed in Morandi et al.[29]

Four infilled specimens tested out-of-plane (TA1, TA2, TA3 and TA4) were previously damaged during the in-plane experiments with the aim of evaluating the reduction of out-of-plane strength related to different levels of in-plane drift. Only the outcomes of the fully infilled specimens have been considered in this work. To assess the out-of-plane strength of the undamaged infill under vertical single-bending and double-bending conditions, two specimens (TA5, TA6), that is, an infill stripe and an undamaged fully infilled configuration, respectively, were tested only out-of-plane. The specimens TA1 to TA5 were subjected to out-of-plane displacement-controlled cyclic tests, whereas TA6 was tested under monotonic load. All the out-of-plane tests have been pushed up to the attainment of ultimate conditions.

TABLE 1 Performed tests and achieved maximum in-plane drift and out-of-plane displacement/force levels

No.	In-plane (%)	Out-of-plane	Configuration
TNT	3.50	–	Bare frame
TA1	1.50	75 mm	Fully infilled
TA2	2.50	75 mm	
TA3	1.00	75 mm	
TA4	1.00	75 mm	Partially infilled
TA5	–	75 mm	Infill stripe
TA6	–	Maximum force	Fully infilled

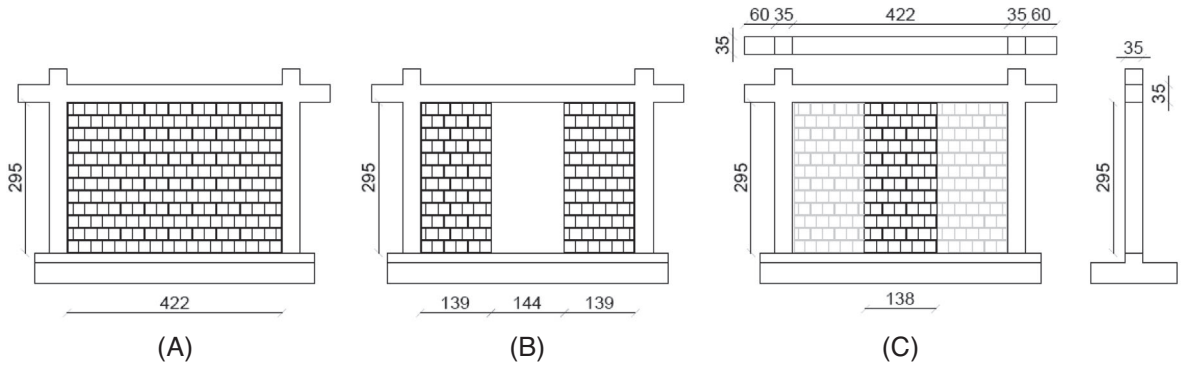

FIGURE 2 Test specimens: (A) fully infilled - TA1, TA2, TA3, TA6; (B) partially infilled – TA4; (C) vertical infill stripe – TA5. Measurements in cm

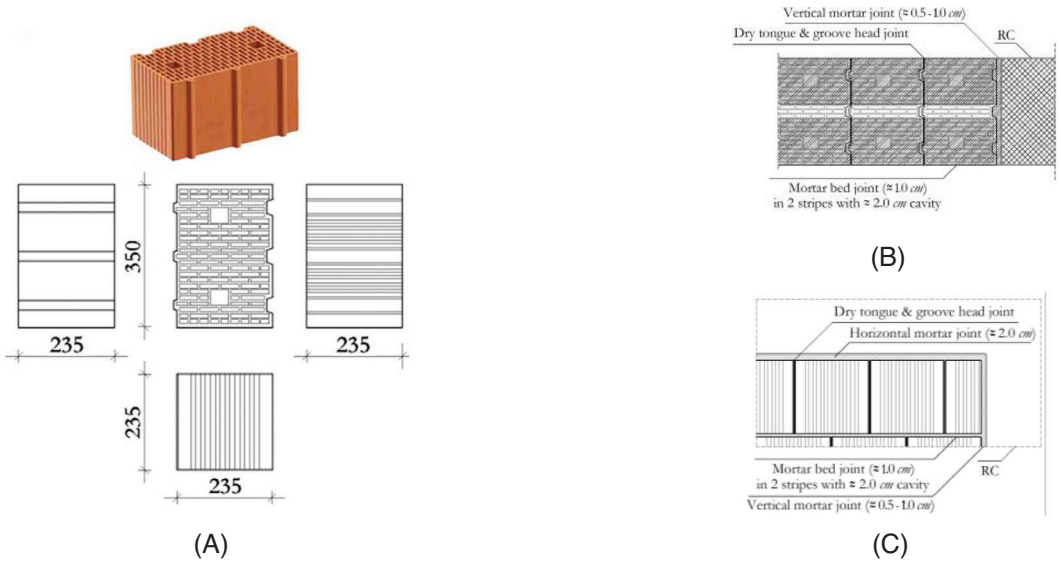

FIGURE 3 (A) Masonry clay units; (B) mortar bed joints; (C) mortar joints adjacent to RC members

The tested infill typology of all the specimens stands for a widely used traditional unreinforced strong clay masonry with lightweight, characterised by vertically hollowed tongue and groove block units (nominal dimensions: 235 × 350 × 235 mm, nominal volumetric percentage of holes: 50%, minimum thickness of webs: 6.8 mm, minimum thickness of shells: 4.8 mm), see Figure 3A. The application of a general-purpose mortar type 'M5' (compression strength of 5.0 MPa) was considered a suitable choice with respect to common construction practise. The specific weight of this masonry typology is 9.40 kN/m^3, with the total weight of the solid infills being equal to about 41 kN. The out-of-plane slenderness λ (infill height over

TABLE 2 Mechanical properties of clay units, mortar and masonry used for the infills

Property	Symbol	Mean (MPa)	c.o.v. (%)
Vertical normalised compression strength of units	$f_{b,\text{norm}}$	9.81	9.2
Lateral normalised compression strength of units	$f'_{b,\text{norm}}$	3.1	10.8
Flexural strength of mortar	f_{fl}	2.15	19.4
Compression strength of mortar	f_{mor}	7.68	20.6
Vertical compression strength of masonry	f_{vert} (f_{mv})	4.64	14.1
Vertical elastic modulus of masonry	E_{vert} (E_{mv})	5299	8.6
Lateral compression strength of masonry	f_{lat}	1.08	14.5
Lateral elastic modulus of masonry	E_{lat}	494	32.8
Initial shear strength of bed-joints	f_{v0}	0.359	26.0

thickness) of the infills is equal to about 8.4. The infills have been constructed after full hardening of the RC frame. Traditional bed joints with a thickness of about 1.0 cm have been applied in two stripes with an intermediate cavity of about 2.0 cm (Figure 3B), and dry head joints have been adopted. Full contact between the infill and the surrounding RC members was assumed to be achieved filling the remaining vertical gaps on the two sides of the infill and the horizontal gap at the top of the infill with mortar (Figure 3C).

The RC frame specimen is meant to represent a single-storey single-bay part of a full-scale RC structure (see Figure 2, sections of the columns and beam: 35 × 35 cm), designed according to European code provisions for new buildings.[21,30,31] More information regarding the design, the dimensions and the reinforcement details of the RC frame are reported in Morandi et al.[29]

Furthermore, a complete characterisation of the relevant properties for all materials utilised for the construction of the specimens has been carried out, as reported in more detail in Morandi et al.,[32] including the evaluation of unit, mortar and masonry properties for the selected infill typology, which are summarised in Table 2.

2.2 | Out-of-plane test setups

The experimental tests were carried out at the laboratory of the Department of Civil Engineering and Architecture of the University of Pavia. Details regarding the test setup, instrumentation and loading protocol for the in-plane experiments can be found in Morandi et al.[29]

During the out-of-plane cyclic static tests, a steel reaction frame illustrated in Figure 4A and B served as a reaction frame for the load being imposed through a servo-controlled hydraulic actuator, restraining at the same time the RC frame in the out-of-plane direction. To transfer the load to the infill, a device consisting of hinged steel beams and plates was used to be able to accommodate the deformed shape of the wall, see Figure 4C and D, and such that the imposed horizontal load could be well distributed at mid-height of the infill.

In the case of specimens TA1, TA2 and TA3, the load was applied in two lines with eight plates for load introduction in each line, resulting in a roughly linear distribution. For specimen TA4 the load was introduced through four plates on each part of the infill, while for specimen TA5 the load was imposed through eight plates.

Such system represents an improvement with respect to most of the out-of-plane test setups used in past studies, which were mainly based on the application of single concentrated loads on the panels (see e.g.,[8,9,14,27]). Further details regarding the adopted out-of-plane setup can be found in Hak et al.[12]

Since the test set-up described previously was expected to cause punching-type local brittle failure in the clay units, the undamaged fully infilled specimen TA6 was subjected to a simple out-of-plane monotonic load test up to collapse. The specimen was overturned horizontally with the vertical direction being the direction of out-of-plane loading (Figure 5A). The RC frame was supported by a series of concrete blocks aiming to achieve an almost continuous vertical support along the perimeter of the frame. The force was applied by placing layers of bags containing dry sand (weight of each bag equal to 25 kg), which covered the whole area of the masonry panel, until collapse was reached (Figure 5B). In the evaluation of the equivalent distributed force over lateral area of the panel, the weight of those parts of sand bags supported directly by the RC elements has not been considered. At the end of placing each layer, the damage pattern was monitored through pictures and measurements of displacement with the instruments that continued to acquire data during the whole duration of the test.

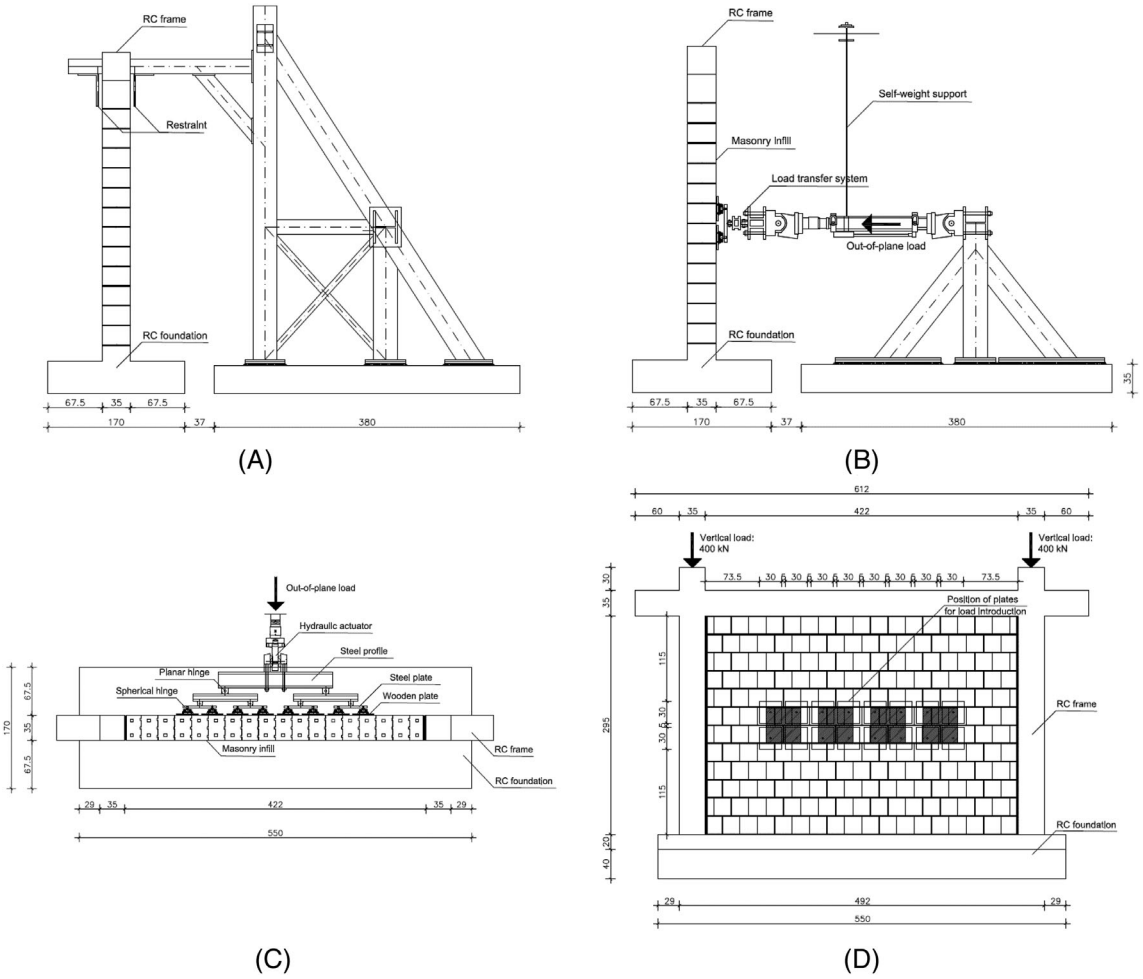

FIGURE 4 Out-of-plane test setup: (A) beam restraining and (B) actuator reaction system; (C) plan view and (D) front view of system for out-of-plane load transfer from actuator to masonry infill. Dimensions in cm

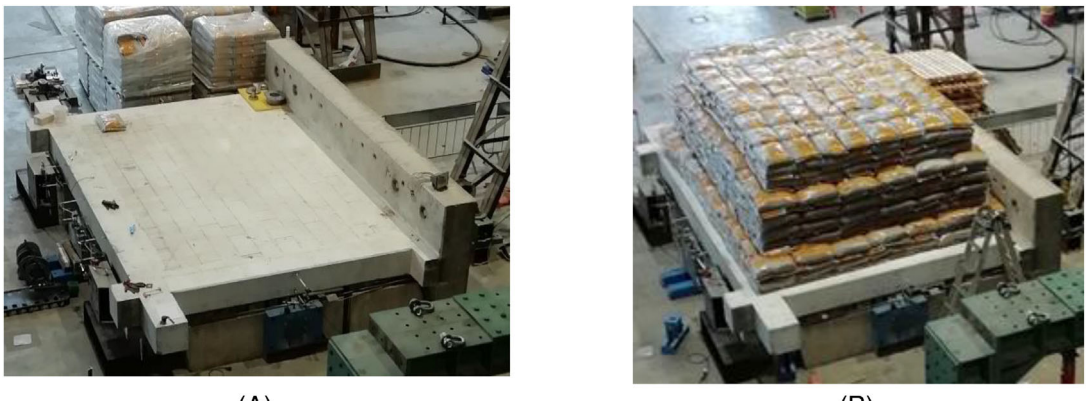

FIGURE 5 Specimen TA6: (A) before the test; (B) load application

Although such systems for load introduction are not able to rigorously reproduce actual seismic forces and dynamic tests on a shaking table are surely the most appropriate solution, the experimental equipment developed and adopted in this research for the application of the out-of-plane action is in line with well-recognised past investigations, provides some additional improvements with respect to similar test setups and represents a rational compromise between the simplicity and costs of the systems and the effectiveness of the results.

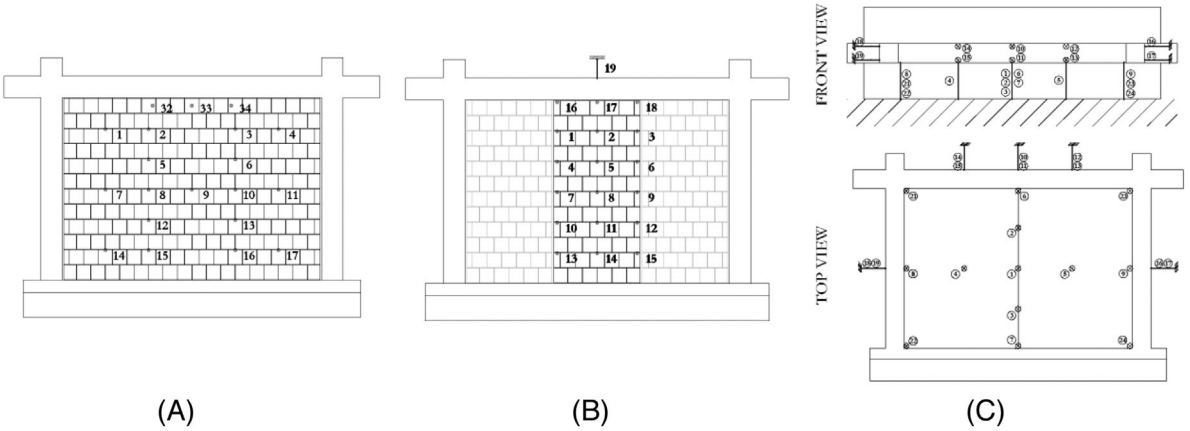

FIGURE 6 Instrumentation layout of (A) TA1, TA2, TA3; (B) TA5 and (C) TA6

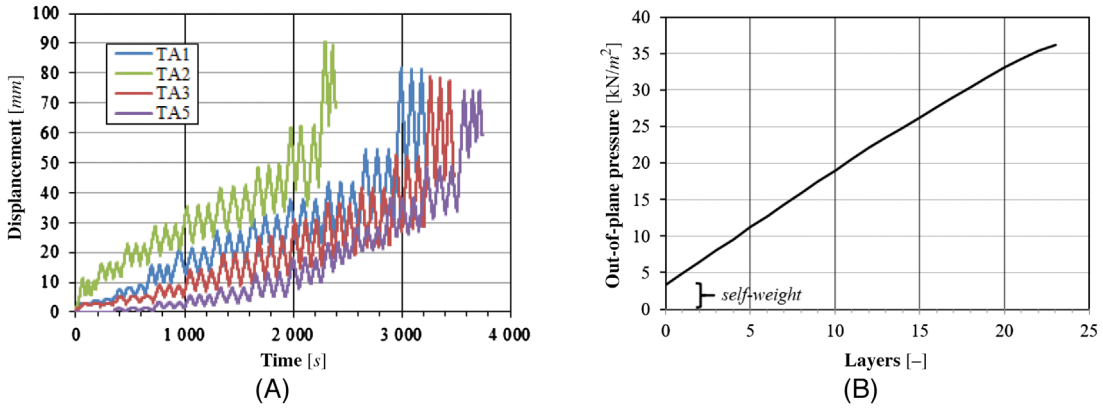

FIGURE 7 Loading protocols: (A) TA1, TA2, TA3, TA5; (B) TA6

2.3 | Instrumentation and loading protocols

To evaluate the out-of-plane displacements (horizontal for TA1 to TA5, vertical for TA6) of the tested infills, displacement transducers (linear potentiometers) were distributed symmetrically throughout the masonry panel, as represented in Figure 6A for TA1, TA2 and TA3, Figure 6B for TA5 and Figure 6C for TA6. At the same time, possible displacements of the surrounding RC frame and the foundation of the specimen were controlled. Additionally, the out-of-plane displacements of the RC frame, the vertical displacements of the top beam and the sliding of the foundation with respect to the strong floor were monitored.

Specimens TA1 to TA5 were tested in the out-of-plane direction applying cycles of horizontal force in one direction (push and back to almost zero force) by means of the actuator, using the steel reaction frame illustrated in Figure 4A and B, after imposing a constant vertical force equal to 400 kN on each RC column through two independent hydraulic jacks, each placed between the column and a rigid transversal steel beam tied down to the foundation with two steel bars. For each level of target loading (i.e., target force at the first two levels of loading and target displacement at subsequent levels of loading), three complete cycles have been accomplished, keeping the duration of each loading level roughly constant. A minimum force had to been maintained during unloading (ca. 5.0 kN) to keep the complete contact between the loading device and the infill. The loading protocols for specimens TA1 to TA5 are reported in Figure 7A. Further details regarding the adopted instrumentation and loading can be found in Hak et al.[12]

The loading protocol for TA6 was based on a typical monotonic increasing load test and was stopped at the collapse of the infill, as shown in Figure 7B.

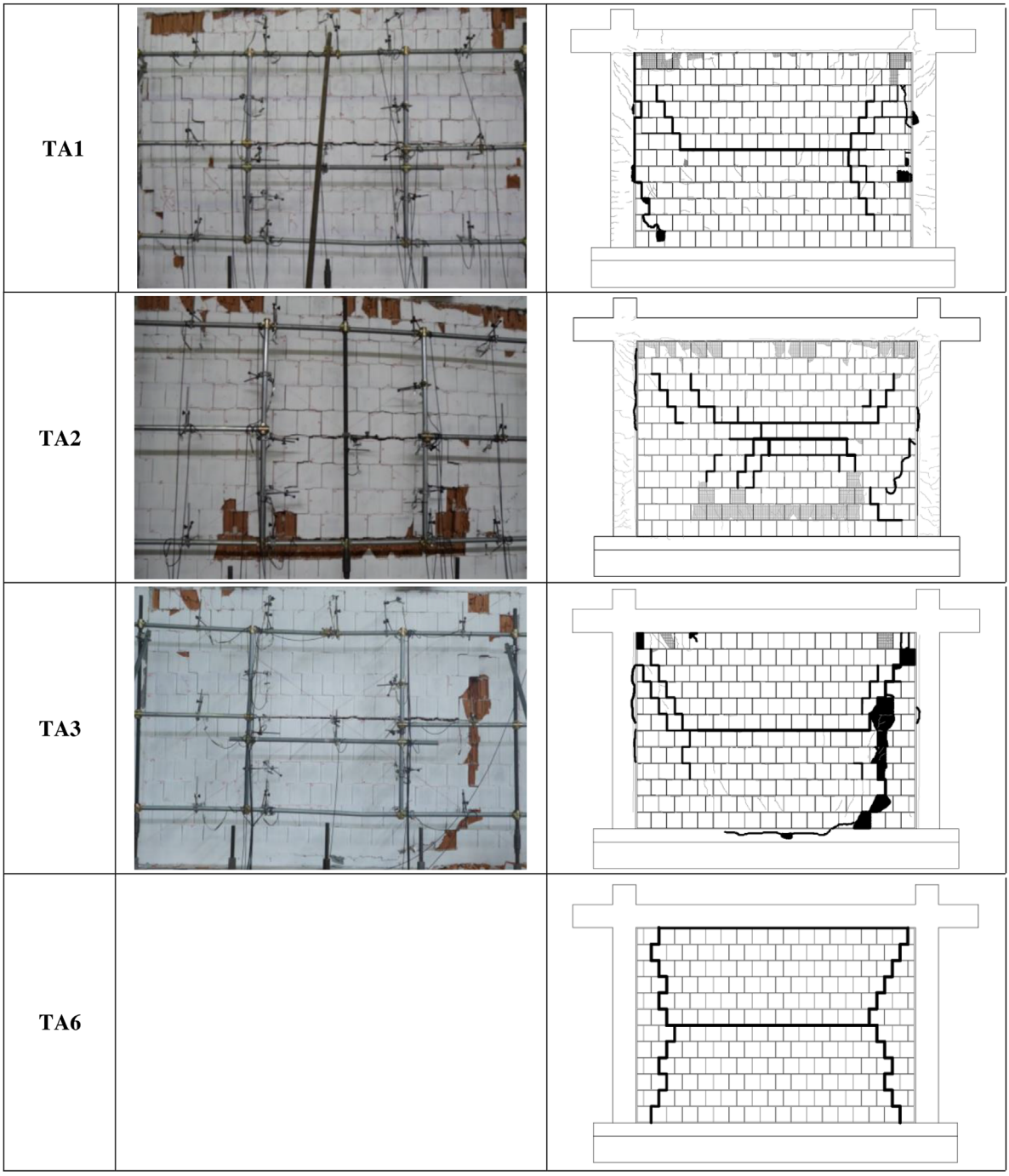

FIGURE 8 Crack pattern at 75 mm target displacement: pictures (left) and sketch (right, in black – out-of-plane damage, in grey – previous in-plane damage)

3 | INTERPRETATION OF OUT-OF-PLANE EXPERIMENTAL RESULTS

3.1 | Damage pattern and deformed shapes

3.1.1 | 'Double bending' infill configurations (TA1, TA2, TA3, TA6)

In order to illustrate the experimentally obtained double bending response of the fully infilled configuration, Figure 8 shows the damage patterns of the previously damaged panels TA1, TA2 and TA3, corresponding to a target displacement

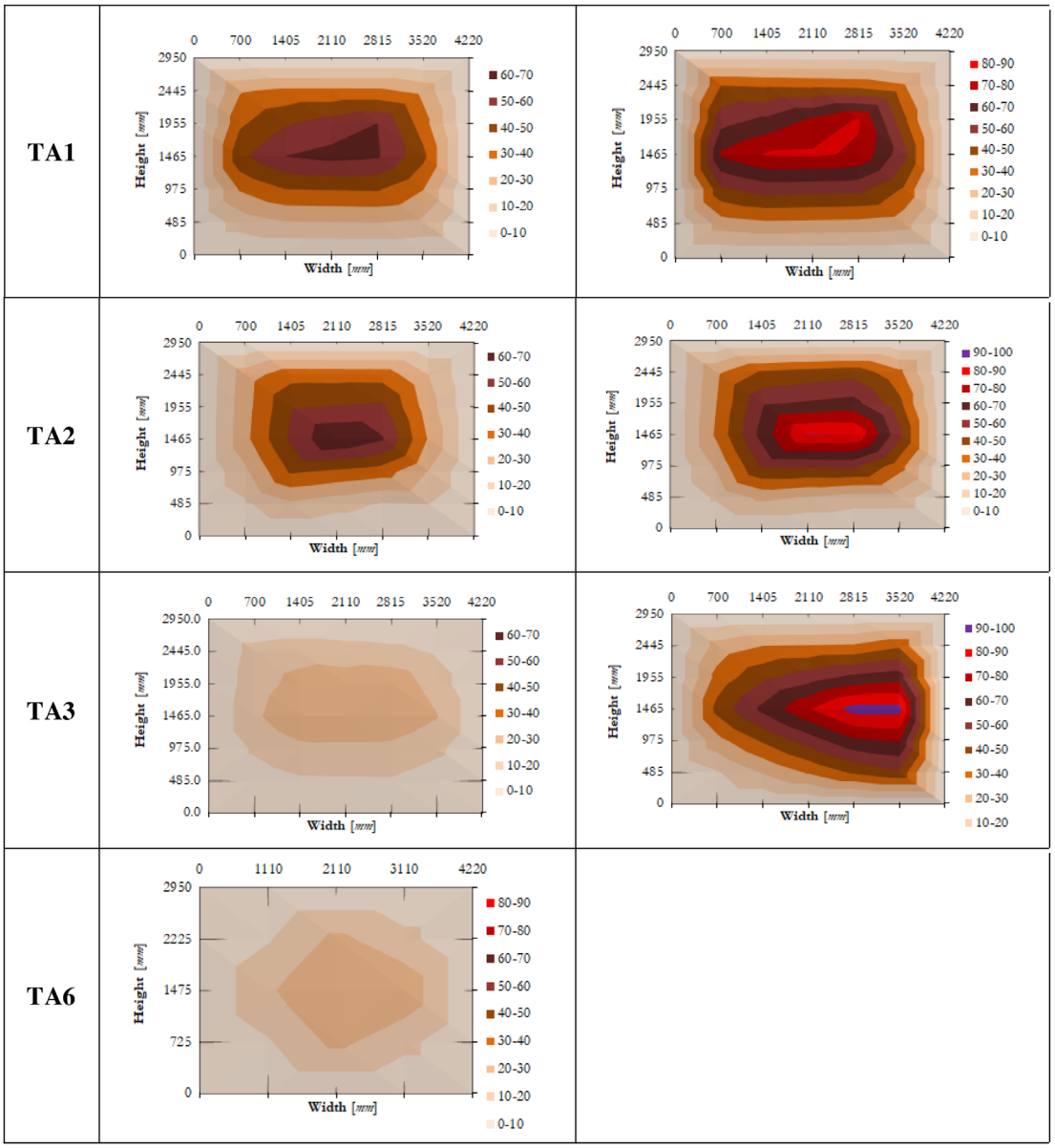

FIGURE 9 Out-of-plane deflection of fully infilled specimens at maximum force (left) and at 75 mm target displacement (right) for TA1, TA2, TA3 and TA6

of 75 mm. Clearly, a dominating horizontal crack at mid-height of the infill and a stepwise cracking, starting from the horizontal crack at mid-height and spreading towards the corners of the infill could be observed. Such damage pattern confirms that, based on the arching action in the horizontal and the vertical direction, a double-bending resistance mechanism could develop. Furthermore, depending also on the distribution of previous in-plane damage, local failure of masonry blocks may occur, in particular where the most pronounced cracks come together. Further details regarding the damage propagation can be found in Hak et al.[12]

Also in the case of TA6, the damage pattern was in line with the other specimens with four-sided supports, as represented in the sketch of Figure 8. The creation of horizontal cracks approximately in the centre of the panel due to the vertical arching mechanism and the detachment and sliding of the infill at the beam-panel interface has been observed. Again, a horizontal crack at mid-height and stepwise cracks spreading diagonally towards the corners were detected. The development of the cracks has been monitored through the use of cameras with an illuminator placed between the strong floor and the specimen.

The deflected shape of the panel related to the maximum achieved force and to the 75 mm target displacement for each of the fully infilled specimens (TA1, TA2, TA3 and TA6) is shown in Figure 9. A linear interpolation has been assumed

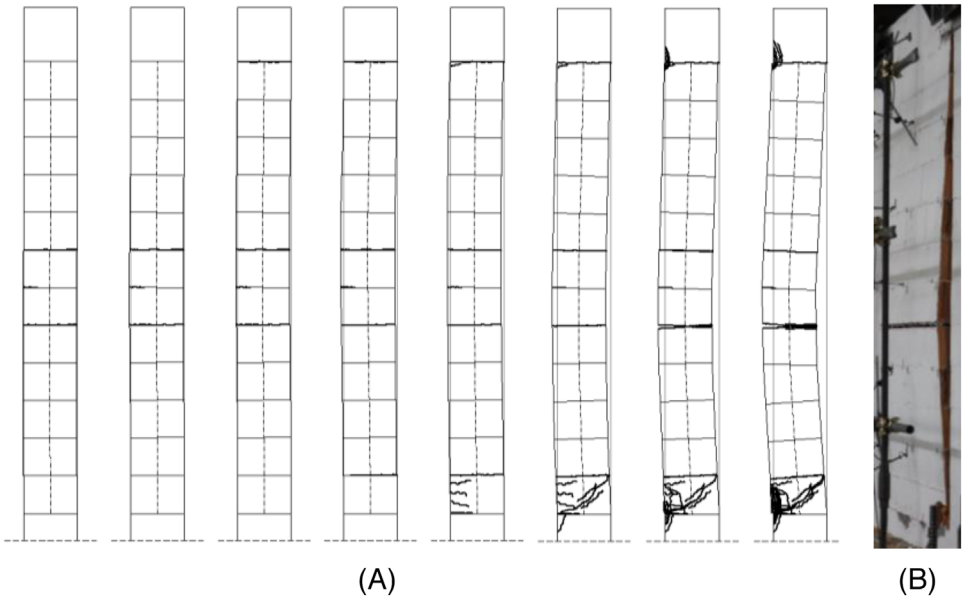

FIGURE 10 Specimen TA5: (A) progression of damage; (B) damage at 75 mm target displacement

between the available points of measurement, when approximating the displaced shapes of the panels based on available data recorded by the potentiometers (see Figure 6A and C). Such response underlines, once again, the formation of a double bending resistance mechanism, based on the out-of-plane arching action in both the horizontal and vertical direction, with a nearly symmetric deflected shape and maximum displacement at the centre of the panels, whilst a more irregular deformation distribution was found only at the highest displacement levels due to the increased damage.

3.1.2 | Single bending infill configuration (TA5)

In order to illustrate the experimentally obtained single bending response of the infill stripe TA5, Figure 10A presents the propagation of damage for a cross section view of the infill. The damaged specimen at the maximum level of out-of-plane displacement equal to 75 mm is shown in Figure 10B.

A main horizontal crack, which occurred at the masonry bed joint below mid-height and the formation of a vertical arching mechanism, could be observed. The response mechanism was apparently achieved through the equilibrium of two rigid bodies, with an upper support at the interface between the infill and the beam, a bottom support at the crack of the first course and the intermediate hinge of the arch at the crack in the mortar joint above the fifth course. Further details regarding the damage propagation during the test TA5 can be found in Hak et al.[12]

3.2 | Out-of-plane force-displacement response and envelope idealisation

The results of the monotonic test for specimen TA6 have been evaluated in terms of pressure (load over lateral infill area ratio) versus displacement, while the results of the cyclic out-of-plane tests for specimens TA1, TA2, TA3 and TA5 have been evaluated in terms of force versus displacement. In both cases, the control point for out-of-plane displacements is placed at the centre of the panel (displacements measured by potentiometer No. 9 for TA1 to TA3, potentiometer No. 8 for TA5 and potentiometer No. 1 for TA6, see Figure 6).

The obtained force-displacement curves and corresponding envelopes for specimens TA1, TA2, TA3 and TA5 are shown in Figure 11A–D, respectively, whereas the monotonic pressure–displacement response for specimen TA6 is reported in Figure 11E. The force–displacement envelopes are once again presented in Figure 11F. For the sake of this comparison, the force levels obtained for TA5 have been multiplied by the length of the solid infill over the width of the stripe (4.22/1.38), in order to consider the response of a solid infill having the same dimensions of the other specimens but characterised by single-bending conditions (here named TA5*). Furthermore, the force levels for TA6 (maximum

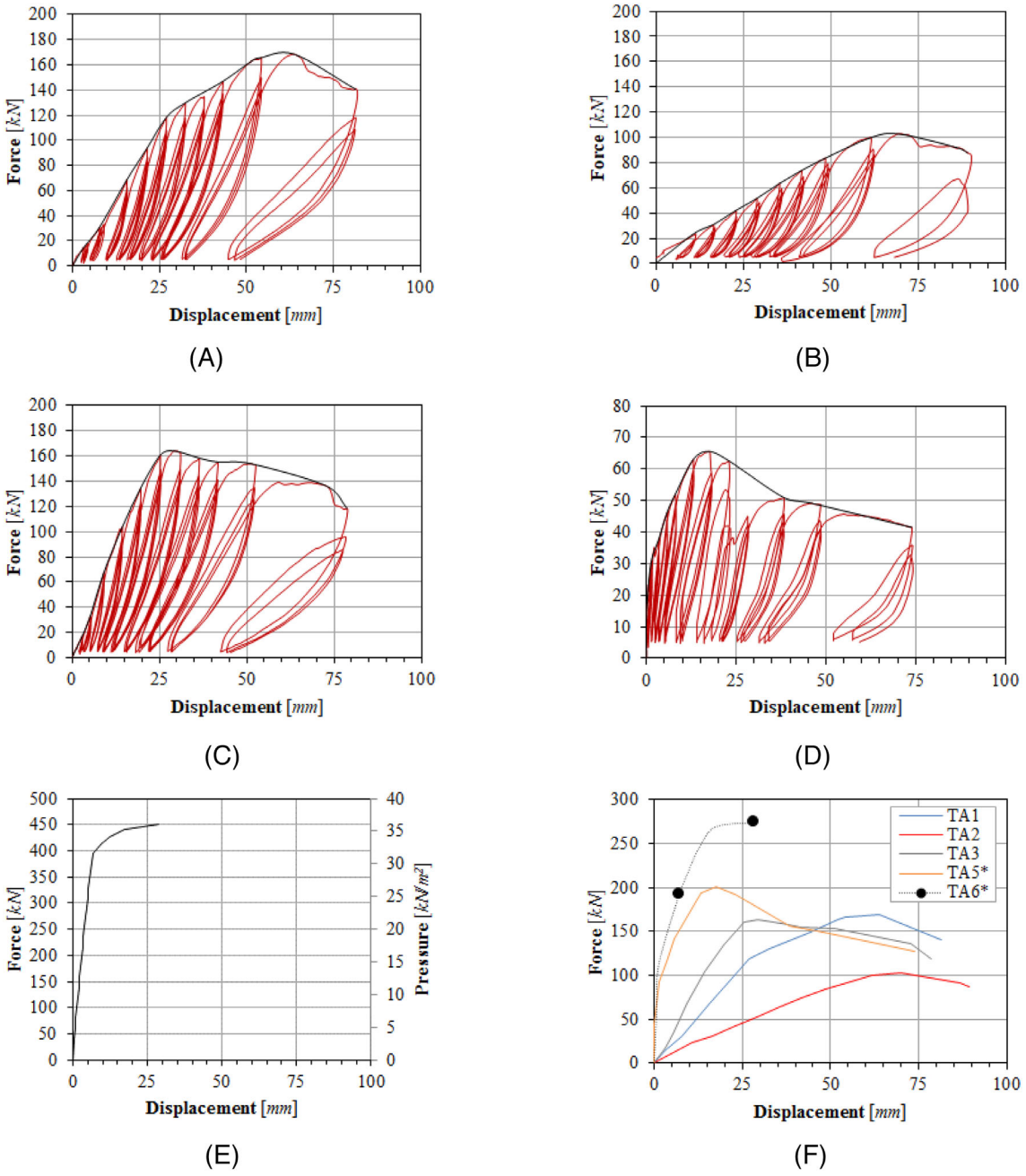

FIGURE 11 Force–displacement response: (A) TA1, (B) TA2, (C) TA3, (D) TA5, (E) TA6 and (F) comparison of the maximum envelopes

pressure and corresponding maximum force, respectively, equal to 36.2 kN/m^2 and 450 kN) have been scaled in order to consistently consider the different loading system with respect to the other specimens and homogenise the forces, using a criterion based on the energy equivalence between TA6 and TA1 to TA3 (see Appendix A). However, it is important to underline that the modified curve TA6*, represented in Figure 11F, has only a qualitative meaning, with the exception of the value of the peak force (F_{max} = 274 kN) and elastic stiffness at 0.7F_{max} (k_{el} = 27 kN/mm), as reported in Appendix A.

A common approach to interpret the force–displacement experimental results and to evaluate the related seismic parameters is to idealise the envelope by means of a bilinear curve. Here, an approach derived from the interpretation of shear-compression tests on load-bearing masonry walls has been used (e.g., see Morandi et al.).[33] Since three loading cycles at each target displacement were carried out in this experimental campaign on TA1 to TA5, three envelopes are obtained. On each envelope, the experimental stiffness k_{el} has been evaluated considering the slope of the secant at 70% of the maximum force of the force–displacement envelope F_{max}, the ultimate displacement d_u as the displacement corresponding to a strength degradation equal to 20% of F_{max}, and the value of the force F_y, corresponding to the horizontal

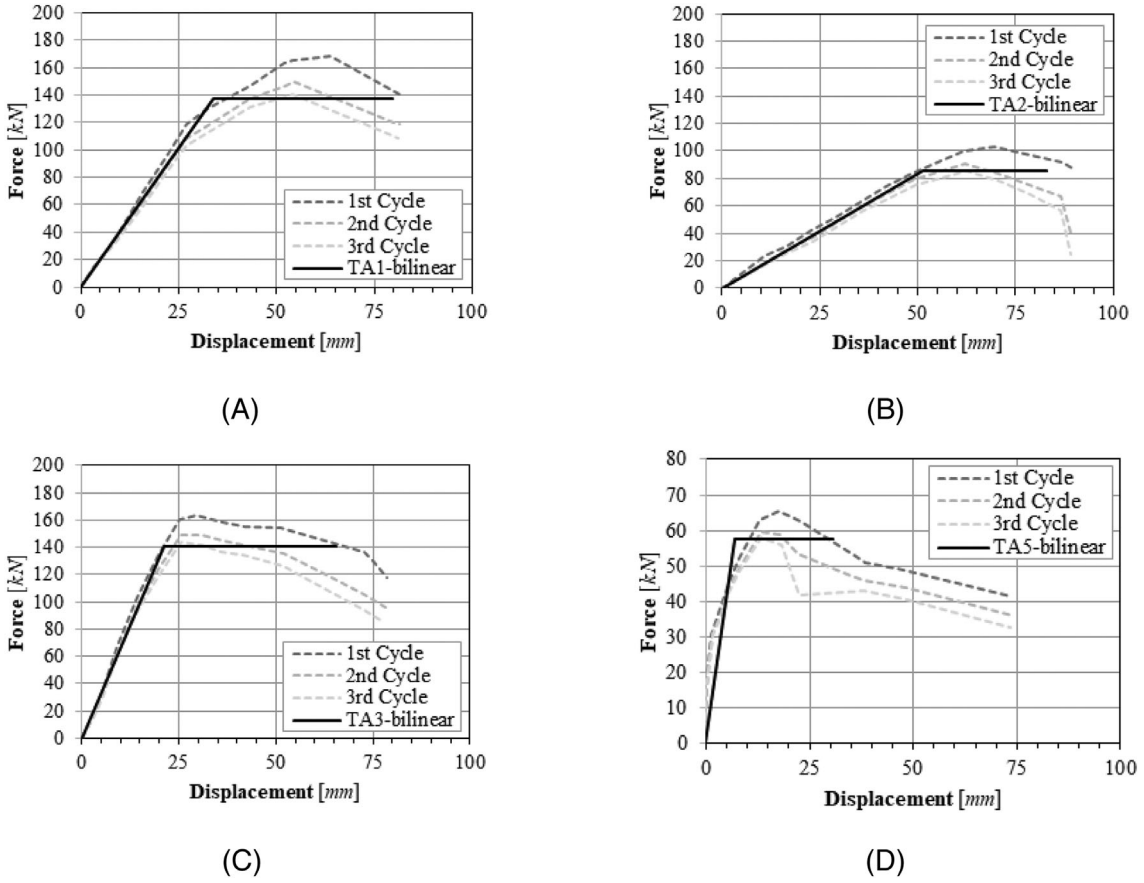

FIGURE 12 Force–displacement envelopes and related bilinear curves: (A) TA1; (B) TA2; (C) TA3 and (D) TA5

TABLE 3 Main seismic equivalent parameters from the envelopes of the out-of-plane tests

	k_{el} (kN/mm)	F_y (kN)	F_{max} (kN)	d_y (mm)	d_u (mm)	μ_c (–)
TA1 (1.5% IP)	4.06 *(4.4; 4.0; 3.8)*	138 *(153; 133; 127)*	168 *(168; 150; 141)*	33.9 *(35; 33; 33)*	79.4 *(81; 80; 78)*	2.35
TA2 (2.5% IP)	1.67 *(1.8; 1.7; 1.6)*	86 *(97; 83; 78)*	103 *(103; 90; 86)*	51.3 *(54; 50; 50)*	83.1 *(89; 82; 78)*	1.62
TA3 (1.0% IP)	6.61 *(7.0; 6.5; 6.3)*	141 *(151; 139; 133)*	164 *(164; 150; 144)*	21.3 *(22; 21; 21)*	65.3 *(75; 63; 59)*	3.07
TA5 (0.0% IP)	8.49 *(8.2; 8.8; 8.5)*	57.7 *(62; 55; 56)*	66.0 *(66; 60; 58)*	6.80 *(7.5; 6.2; 6.6)*	30.6 *(36; 34; 21)*	4.50
TA5* (0.0% IP)	26.0 *(25; 27; 26)*	176 *(188; 168; 171)*	200 *(200; 182; 178)*	6.80 *(7.5; 6.2; 6.6)*	30.6 *(36; 34; 21)*	4.50
TA6* (0.0% IP)	27.0	—	274	–	–	–

Note: the values in brackets correspond to the parameters of each of the three cycles; F_{max} is the maximum of the three values.

branch of the bilinear curve, ensuring that the areas below the cyclic envelope curve and below the equivalent bilinear curve up to d_u are equal. From the results of the three cycles, a single equivalent bilinear curve has been determined, taking the average of the three values of k_{el}, F_y and d_u. The 'yield' displacement d_y has been set equal to F_y/k_{el} and the ductility capacity μ_c equal to d_u/d_y. The so calculated bilinear curves are illustrated in Figure 12 along with the three envelopes, while Table 3 summarises the seismic parameters for all the considered specimens. The value of the elastic stiffness for TA6* is evaluated through the method described in Appendix A.

In the interpretation of such results, it is important to underline that the test on TA6 was carried out with monotonic loading and without vertical loads on the RC columns, differently by the other tests which were conducted with cyclic actions and vertical loads on the columns. However, the out-of-plane strength and stiffness parameters are not expected to be significantly reduced by the cyclic loading as respect to the monotonic, as also shown in the tests by Furtado et al.[11] Moreover, the application of the vertical loads on the columns should not affect considerably the out-of-plane behaviour of the masonry panel if the deflection of the upper beam, which could provide additional vertical stress on the masonry, is negligible, as in the tested specimens; for this reason, some out-of-plane tests were also carried out without any vertical load on the columns of the RC frame (see, e.g., Palieraki et al.[13] and Di Domenico et al.[10]).[1]

The results of the force–displacement envelopes in Figure 11F and of the seismic parameters demonstrate clearly the significant degradation of stiffness and strength in the out-of-plane direction for increasing values of previous in-plane drift and related damage, in particular for relatively high levels of drift and extensive preceding damage. The undamaged in-plane specimens TA6* and TA5* have provided, as expected, larger values of elastic stiffness and strength, with the latter achieving lower values since it was tested under vertical single-bending. Specimens TA3 and TA1 obtained almost equal values of peak resistance (163.9 and 168.5 kN, corresponding to 1.0 % and 1.5 % previous in-plane drift, respectively); however, for specimen TA1 a more pronounced stiffness degradation has been observed (about 60% of the one of TA3). These specimens also showed severe degradation with respect to TA6*, in strength (60% and 61% of the one of TA6*, respectively) and in stiffness (24% and 15% of the one of TA6*, respectively). The peak resistance and the stiffness of specimen TA2 have dropped to 102.7 kN and to 1.67 kN/mm, respectively, equal to about 37% and 6% of the ones of specimen TA6. Finally, the out-of-plane ductility capacity is also reduced for increasing values of previous in-plane drift.

4 | OUT-OF-PLANE STRENGTH AND STIFFNESS REDUCTION IN FUNCTION OF IN-PLANE DAMAGE

The experimental values of out-of-plane resistance obtained following the in-plane tests (i.e., at 0.0%, 1.00%, 1.50% and 2.50% in-plane drift) are shown in Figure 13 and summarised in Table 4, along with the fraction of the corresponding value obtained for the undamaged panel, resulting in the experimentally evaluated out-of-plane strength reduction coefficient $\beta_{R,\text{exp}}$. For each test, the considered force is the peak value of the maximum envelope.

After a first reduction of the out-of-plane resistance, the strength remains substantially constant up to a drift of about 1.50%–1.75%, then followed by a soft degradation similar to the one of the first branch up to the maximum applied drift (2.50%).

The Figure 14 and the values of Table 4 report the trend of the experimental out-of-plane elastic stiffness computed as defined in Section 3.2 (Table 3) in function of the in-plane drift, along with the ratio of the corresponding value obtained for the undamaged panel, that is, the out-of-plane stiffness reduction coefficient $\beta_{k,\text{exp}}$. The results show a sharp degradation from 0.0% to 1.0%, with a softer decrease from there on, proving that the main loss of stiffness occurs at small values of in-plane drift, when the wall begins to be damaged and to be detached from the frame. It is important to underline that the variation of the elastic stiffness can strongly affect the seismic out-of-plane verification, since it modifies the fundamental out-of-plane period of the infill and, therefore, the pressure/force acting on the panel.

The results of the out-of-plane strength reduction obtained for the considered strong infill typology have been compared with those of different combined in-plane/out-of-plane tests carried out in the past on various clay infill typologies with variable thickness and slenderness (infill height h_w over thickness t_w), mostly referring to structures designed according to modern seismic design provisions, as reported in Figure 15. The tests by Calvi and Bolognini[8] and Ricci et al.[14] were both performed on masonry panels with thin horizontally hollowed clay blocks, being the former carried out on 1:1 scaled 12 cm thick specimens (h_w/t_w 20.4), while the latter on 2:3 scaled 8 and 12 cm thick walls (h_w/t_w = 22.9 and 15.2). Angel et al.,[7] experimented very slender infills with solid clay bricks having a thickness of 10 cm (h_w/t_w = 33.9) and Furtado et al.,[25] performed real scale tests on thicker clay masonry panels with horizontal holes (t_w = 15 cm and h_w/t_w = 15.3). Finally, da Porto et al.[9] carried out 1:1 scale experiments on strong modern masonry infills built with vertically hollowed clay units having a thickness of 30 cm (h_w/t_w = 8.8), similar to the typology considered in this study.

The different thickness and slenderness of the infills clearly play a major role in the reduction coefficient/in-plane drift response, as already pointed out by different authors (e.g.,[12,14,23]). As expected, with reference to Figure 15, the extent of the out-of-plane strength degradation is more pronounced on slender/weak infills in particular if realised with highly perforated blocks with horizontal holes, which proves that thicker infills present a lower resistance reduction thanks to better in-plane performance, that is, to lower levels of damage due to in-plane actions. The reduction coefficient $\beta_{R,\text{exp}}$ obtained for the infill in this study is the largest (corresponding to the lowest reduction) in comparison to previous test results from literature, also slightly above the one corresponding to the other strong infill typology tested by da Porto et al.,[9] which, anyhow, had a higher slenderness compared to the one of this study (8.8 versus 8.4). Moreover, the reduction coefficient in da Porto et al.[9] was not defined experimentally, but derived computing the out-of-plane resistance of the undamaged panel through an analytical approach (see[24,27]).

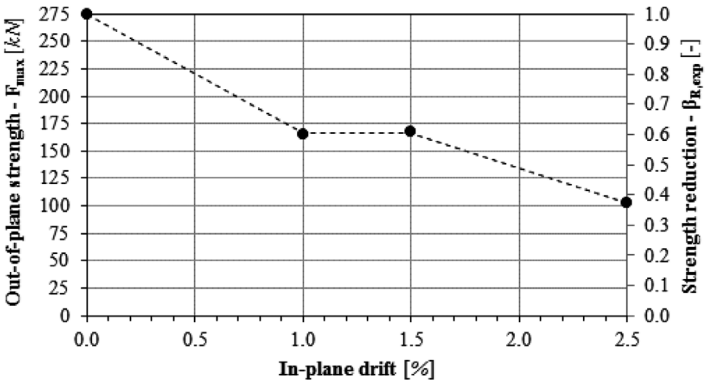

FIGURE 13 Experimental out-of-plane resistance and reduction coefficient $\beta_{R,exp}$ in function of previous in-plane drift

TABLE 4 Experimental out-of-plane resistance, stiffness and reduction coefficients $\beta_{R,exp}$ and $\beta_{k,exp}$ in function of previous in-plane drift for strong infill

In-plane drift (%)	F_{max} (kN)	$\beta_{R,exp}$ (–)	k_{el} (kN/mm)	$\beta_{k,exp}$ (–)
0.00	274	1.00	27.0	1.00
1.00	164	0.60	6.61	0.24
1.50	168	0.61	4.06	0.15
2.50	103	0.37	1.67	0.06

A similar comparison of the presented results with past experimental campaigns in terms of the elastic stiffness degradation is difficult and could lead to inconsistencies in the interpretation, since the approaches adopted by the various authors for the estimation of the initial stiffness are significantly different.

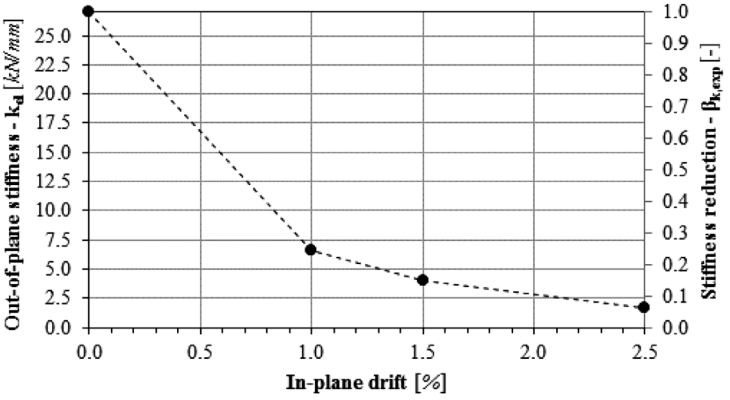

FIGURE 14 Experimental out-of-plane stiffness and reduction coefficient $\beta_{k,exp}$ in function of previous in-plane drift

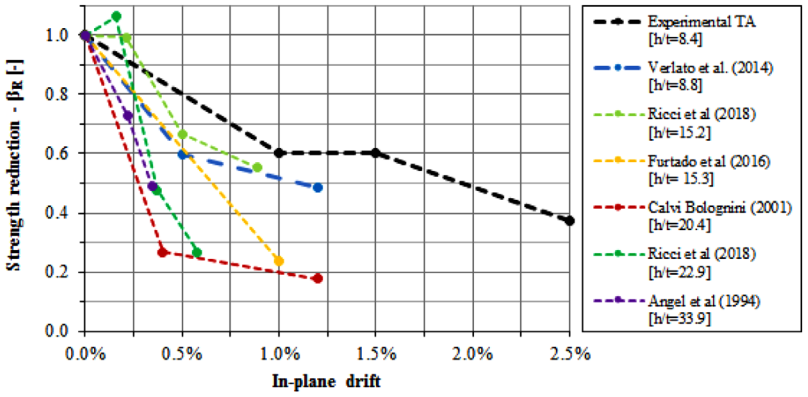

FIGURE 15 Out-of-plane strength reduction in function of in-plane drift: comparison with different masonry infill typologies

5 | IMPLICATIONS FOR OUT-OF-PLANE DESIGN/ASSESSMENT OF INFILLS

5.1 | Reduction factors for out-of-plane strength and stiffness

Even though only limited data is currently available, resulting in three values of reduced strength and stiffness at three levels of previous damage, observations on the test results indicate that for the estimation of the out-of-plane resistance and stiffness, an experimental reduction may be assumed, descending for increasing levels of previously imposed in-plane drift, as illustrated in Figures 13 and 14 and resumed in Table 4.

Subsequently, considering the need to adopt for possible design applications a simple but effective approach, the out-of-plane strength reduction coefficient β_R may be defined in function of the expected in-plane drift demand δ_w of the infilled frame, expressed by simplified relations, for example, by a linear reduction by parts (trilinear) given in Equation (1) or by a polynomial interpolation, as represented in Figure 16A and B. In the definition of β_R, the minimum between the values corresponding to the in-plane drifts at 1.00% and 1.50% has been assumed (=0.60).

Based on the same approach, on the basis of the results of Figure 14, the out-of-plane stiffness reduction coefficient β_k may be defined in function of the in-plane drift demand δ_w, following the bi-linear reduction of Equation (2) or the polynomial interpolation, as represented in Figure 16A and B.

$$\beta_R = \begin{cases} \left(r_{R,1} - 1\right) \cdot \dfrac{\delta_w}{\delta_{\mathrm{DLS}}} + 1 & \delta_w \le \delta_{\mathrm{DLS}} \\ r_{R,1} & \delta_{\mathrm{DLS}} < \delta_w \le \delta_{\mathrm{ULS}} \\ 0\,;\ \left\{ \dfrac{\left(r_{R,2} - r_{R,1}\right)}{\left(\delta_{\mathrm{ULS}} - \delta_{\max}\right)} \cdot \left(\delta_{\mathrm{ULS}} - \delta_w\right) + r_{R,1} \right\} & \delta_{\mathrm{ULS}} < \delta_w \end{cases} \tag{1}$$

$$\beta_k = \begin{cases} \left(r_{k,1} - 1\right) \cdot \dfrac{\delta_w}{\delta_{\mathrm{DLS}}} + 1 & \delta_w \le \delta_{\mathrm{DLS}} \\ \left\{ \dfrac{\left(r_{k,2} - r_{k,1}\right)}{\left(\delta_{\mathrm{DLS}} - \delta_{\max}\right)} \cdot \left(\delta_{\mathrm{DLS}} - \delta_w\right) + r_{k,1} \right\} & \delta_{\mathrm{DLS}} < \delta_w \end{cases} \tag{2}$$

These simplified relations depend on the values of in-plane drift δ_{DLS} and δ_{ULS}, which correspond to the attainment of damage limitation and ultimate limit state conditions (life safety/severe damage), and on the remaining fraction of out-of-plane strength and stiffness $r_{R,1}$, $r_{k,1}$ and $r_{R,2}$, $r_{k,2}$ corresponding respectively to δ_{DLS} and δ_{ULS}. The drift limits δ_{DLS} and δ_{ULS} have been estimated on the results of the in-plane tests according to the actual observed damage at the two performance states, as defined in Morandi et al.[29] The aforementioned values, along with the maximum drift value attained during the tests $\delta_{\max}$, are summarised in Table 5. A similar interpretation of experimental results was previously accomplished for the case of unreinforced and lightly reinforced slender/weak clay masonry infills.[23]

Note that, after exceeding the drift corresponding to the achievement of infill ultimate limit state conditions δ_{ULS}, zero out-of-plane strength is assumed and therefore there is no need of performing any further safety checks in terms of in-plane drift at ULS in addition to the one at Damage Limit State already prescribed in the norms, because it is implicitly included in the out-of-plane verification.

In order to carry out the out-of-plane safety verification for masonry infills complying with European seismic code regulations, the proposed out-of-plane strength and stiffness reduction coefficients β_R and β_k may be applied to estimate the reduced out-of-plane resistance and stiffness, accounting for a certain level of previous in-plane damage that is likely to be sustained by the infill. Given that the infill resistance verification is commonly carried out at the ultimate limit state (life safety/severe damage), the corresponding expected in-plane drift, δ_w, consequently needs to be evaluated. Since the design of masonry infilled RC structures is commonly carried out on bare frame structural configurations, the assessment of the related drift demands for the infilled structure may not be a straightforward task. In everyday design practice, the requirement to carry out detailed analyses on the infilled configuration may be rather demanding due to a series of complex issues, such as the nonlinear behaviour of the masonry and uncertainties related to the relevant material properties. However, if for the evaluation of the out-of-plane infill strength reduction the design drift of the bare frame configuration

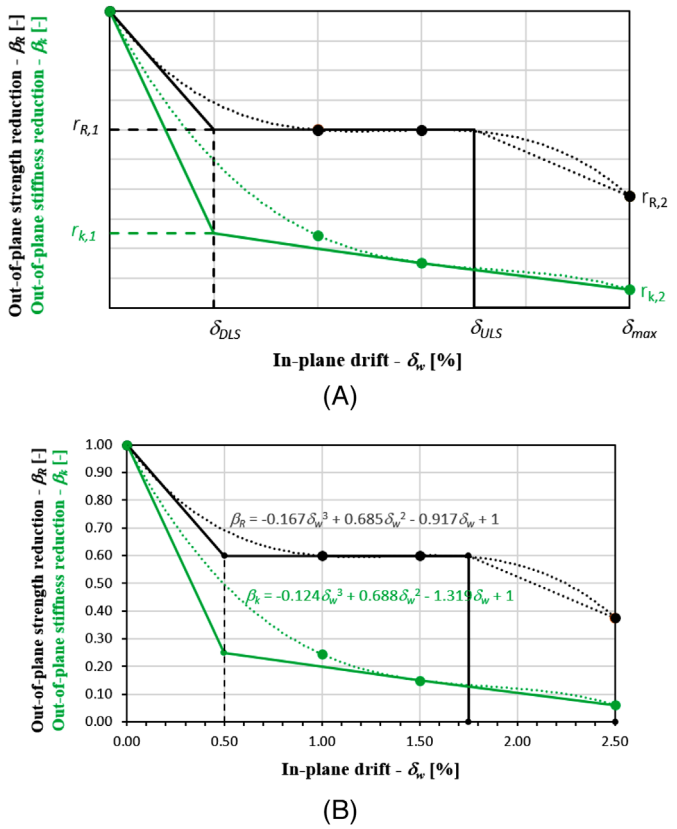

FIGURE 16 (A) Main parameters for the evaluation of the out-of-plane strength and stiffness reduction coefficients β_R and β_k; (B) strength and stiffness reduction coefficient β_R and β_k for strong masonry infill

TABLE 5 Estimated drifts at damage δ_{DLS} and ultimate limit state δ_{ULS}, maximum attained drift δ_{max} and assumed fraction of out-of-plane resistance $r_{R,1}$ and $r_{R,2}$ and stiffness $r_{k,1}$ and $r_{k,2}$

δ_{DLS} (%)	0.50	$r_{R,1}$ (–)	0.60	$r_{k,1}$ (–)	0.25
δ_{ULS} (%)	1.75				
δ_{max} (%)	2.50	$r_{R,2}$ (–)	0.37	$r_{k,2}$ (–)	0.06

is assumed, the given procedure may be overly conservative, since reduced drift demands are expected for the corresponding infilled frame. Hence, for the prediction of the expected drift demands of the infilled frame it may be convenient to apply the simplified procedure proposed by Hak et al.,[34] that is based on the response of the corresponding bare configuration and considers a posteriori the stiffening effects of the infills in function of a simple parameter accounting from the structural characteristics and the properties and amount of the infills.

5.2 | Out-of-plane resistance of the undamaged panel and safety verifications

The proposed relation between the in-plane drift and the out-of-plane strength reduction coefficient β_R cannot be taken as reference unless a proper estimation of the out-of-plane resistance of the undamaged panel (i.e., at 0.0% in-plane drift) is provided, in order to avoid the risk to under- or over-estimate the actual strength, even if the reduction coefficient was consistently calibrated with the experimental results.

The evaluation of the out-of-plane resistance of the considered strong undamaged infill (TA6) has been carried out in the study by Milanesi et al.[35] starting from the ideal one-way vertical arching mechanism with reference to the model by Drysdale et al.,[36] that assumes full contact between the infill and the surrounded frame and neglects the lateral rise at mid-height of the panel. Proper reduction coefficients to consider the decrement as respect to the ideal case due to the effects observed in the tests, namely, the 'second order effects' (deflection of the arch under the lateral load), the deformability

of the frame (uplift of the beam) and the sliding of the panel at the frame/infill interface, have been introduced, along with an incremental coefficient to account for the contribution of the bi-axial bending in the case of infills supported on three/four edges (as TA6). Despite second order effects are usually overlooked in the calculation of out-of-plane resistance of thick panels, the deflection of the arch under lateral loads cannot be disregarded, being not always negligible for robust infills, as reported in Milanesi et al.,[35] above all if the lateral displacement produced by the rotation of the two sub-panels activing the three-pinned arch mechanism is amplified by possible deformation of the surrounding frame (e.g., top beam).

An out-of-plane shear verification has also been proposed to account for possible local shear failure/crushing of masonry units at the edges of the panel which, if occurred, would not allow or would limit the full development of the arching mechanism.

Therefore, the expression of Equation (3) defined in terms of lateral pressure w_R, which modifies the common expression corresponding to a full vertical arching mechanism with the introduction of reduction coefficients accounting for the out-of-plane deflection ($k_{P\Delta 0}$), flexible supports ($k_{P\Delta g}$) and possible sliding of the panel (k_{SL}), is considered to be consistent with the experimental results and sufficiently conservative for design/assessment procedures, as reported in Milanesi et al.[35] An increasing coefficient related to the bi-directionality of the out-of-plane response (k_{BD}) may also be included in the expression and can be estimated as the ratio between the vertical bending moment of a simple supported beam and the vertical moment of a plate calculated through the theory of the elastic orthotropic plates.

$$w_R = k_{P\Delta 0}\, k_{P\Delta g} k_{\mathrm{SL}} k_{\mathrm{BD}} 0.72 \left(\frac{t_w}{h_w}\right)^2 f_d \tag{3}$$

where t_w and h_w are the thickness and the height of the infill panel and f_d is the design compression strength of the masonry set as the ratio between the characteristic value (in the design) or the mean value (in the assessment) of the compression strength and the material safety factor γ_M for the seismic action combination. Values of $k_{P\Delta 0} = 0.95$, $k_{P\Delta g} = 0.95$, $k_{\mathrm{SL}} = 0.80$ and $k_{\mathrm{BD}} = 1.00$ and $\gamma_M = 1.0$ well-predict the TA6 experimental response, being the resisting lateral pressure w_R computed according to Equation (3) equal to 34.0 kPa, while the maximum experimental pressure equals to 36.2 kPa.

In design procedures, the values of the coefficient should be suitably defined according to the actual situation. For example, if the frame cannot deform, for example, for the presence of infills at the upper and lower storey that limit the deformation of the beams and/or for beams heavily loaded, $k_{P\Delta g}$ can be taken equal to 1.0. Then, if the panel/frame interface joint is fully filled at the boundaries and/or suitable out-of-plane restraints are realised, the out-of-plane sliding at the panel/frame interface is unlikely or can be limited and therefore, it could be reasonable to assume values of k_{SL} larger than 0.80 (up to 1.00 if the sliding is completely inhibited). On the other hand, a reduction coefficient due to second-order effects $k_{P\Delta} = k_{P\Delta 0} \cdot k_{P\Delta g}$ at least equal to 0.90 is always strongly recommended for such thick masonry infills. Finally, the bi-directionality of the out-of-plane response can be conservatively neglected ($k_{\mathrm{BD}} = 1.00$), above all when the lateral restraints are not clearly effective or present or in case of full-height openings.

As an alternative, Equation (3) can be modified into Equation (4), where the second-order effects are considered explicitly with the introduction of the central deflection of the arch Δ which, for such strong masonry infill, can be conservatively taken as $0.10 t_w$. Other values of Δ, to be expressed in terms of wall thickness ratio, can be derived for different masonry typologies.

$$w_R = k_{\mathrm{SL}}\, k_{\mathrm{BD}} \frac{0.8 t_w\,(0.9\, t_w - \Delta)}{h_w^2}\, f_d = k_{\mathrm{SL}}\, k_{\mathrm{BD}} \frac{0.8 t_w\,(0.9\, t_w - 0.1\, t_w)}{h_w^2} f_d \tag{4}$$

Therefore, once the strength of the undamaged panel (w_R) is evaluated, the out-of-plane resistance of a damaged infill ($w_{R,\beta}$) can be found in a simplified manner from Equation (5), reducing w_R applying the corresponding reduction coefficient β_R.

$$w_{R,\beta} = w_R \cdot \beta_R \tag{5}$$

Thus, in force-based design/assessment procedures, in order to satisfy the out-of-plane resistance verification for a masonry panel that is expected to sustain a certain level of in-plane damage, the seismic force F_a, expressed as equivalent pressure w_a in Equations (6) acting on the masonry infill, needs to be smaller than the corresponding out-of-plane

resistance $w_{R,\beta}$ (Equation (7)).

$$F_a = \frac{S_a \cdot W_a}{q_a} \;;\; w_a = \frac{F_a}{h_w \cdot L_w} \tag{6}$$

$$w_a \leq w_{R,\beta} \tag{7}$$

In Equations (6), S_a is the out-of-plane seismic acceleration demand normalised to g applicable to the panel, W_a the corresponding weight and q_a is the behaviour factor of the panel having height h_w and length L_w.

5.3 | Out-of-plane period of the infill

Several expressions have been proposed for the evaluation of the out-of-plane acceleration demand on non-structural elements (e.g.,[37,38]) and are included in the Norms (e.g., EC8[21], Instructions of NTC18, MIT, 2019[39]). All these expressions depend, among the other parameters, on the value of the out-of-plane period of the infill T_a, which, in turn, depends on the elastic stiffness, function of the in-plane drift demand δ_w. For the evaluation of the out-of-plane natural elastic period of an infill adherent to the frame, different formulations may be used, some of them being rather burdensome for designers in the case of four-sided supports and orthotropic materials. However, simplifications can be made if the panel may be modelled as a simply supported element (top and bottom supports), which is reasonable if applied on the considered infill, where the horizontal stiffness is much lower than the vertical one (see[35]). Therefore, the out-of-plane natural elastic period of an infill can be conservatively evaluated using the expression in Equation (8) for simply supported vertically spanned elements of height h_w, obtained by the theory of systems with distributed mass and elasticity, neglecting damping and assuming a shape function as $\psi(x) = \sin(\frac{\pi x}{h})$.[40]

$$T_a = 2\pi \sqrt{\frac{\tilde{m}}{\beta_k \tilde{k}}} = \frac{2\, h_w^2}{\pi} \sqrt{\frac{m}{\beta_k (\alpha_{cr} E_{mv} I)}} \tag{8}$$

Parameters $\tilde{m}$ and $\tilde{k}$ are the generalised mass and stiffness of the infill, m the mass per unit of height h_w, E_{mv} the vertical modulus of elasticity of the masonry, I the out-of-plane moment of inertia ($=L_w t_w^3/12$), α_{cr} the cracking coefficient of the elastic stiffness and β_k is the out-of-plane stiffness reduction coefficient given in Equation (2) and Figure 16 as a function of the in-plane drift. The out-of-plane elastic stiffness of masonry infills should be considered cracked, in order to account for the influence of cracking on deformations and to better approximate the slope of the first branch of the bi-linear force-deformation model, as also indicated in EC8 for structural masonry. The common value of the cracking coefficient α_{cr} equal to 0.50 may be used, although for this strong infill a lower value ($\alpha_{cr} = 0.27$) has been found through numerical simplified analyses (see Appendix A).

According to Equation (8), the increase of the period is therefore proportional to the square root of the inverse of β_k. As reported in Figure 17 and Table 6, the out of-plane elastic period of the considered infill, calculated with β_k given by Equation (2) and with a cracking coefficient α_{cr} equal to 0.27, has provided an increasing trend as a function of the in-plane drift of about two times at 0.50% drift and four times at 2.50% drift.

5.4 | Out-of-plane behaviour factor of the infill

In the context of the force-based approach for the out-of-plane safety verifications on masonry infills, the evaluation of the behaviour factor of the infill, q_a, plays a fundamental role.

The rigorous method to derive q_a should be based on the execution of non-linear dynamic analyses applying floor accelerograms on the out-of-plane response calibrated on the test results. The values of q_a can be then computed as the ratio between the seismic force that the element would experience if its response was completely elastic, and the maximum seismic force that may be used in the design with a conventional elastic analysis model, still ensuring a satisfactory response of the infill (i.e., the deformation capacity is not exceeded).

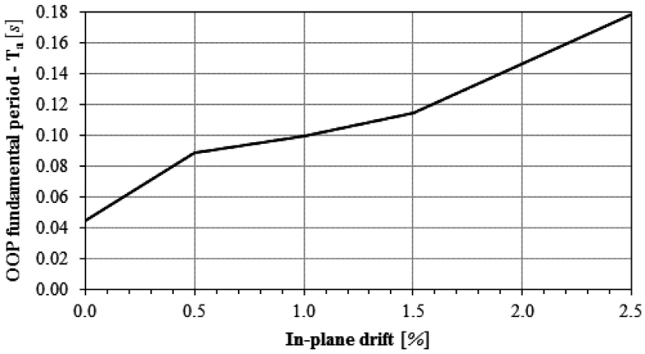

FIGURE 17 Out-of-plane fundamental period T_a in function of previous in-plane drift

TABLE 6 Out-of-plane fundamental period T_a and amplification factor ($\beta_k^{-0.5}$) in function of previous in-plane drift

In-plane drift (%)	$\beta_k^{-0.5}$ (–)	T_a (s)
0.00	1.00	0.044
0.50	2.00	0.088
1.00	2.24	0.099
1.50	2.58	0.114
2.00	3.16	0.139
2.50	4.08	0.180

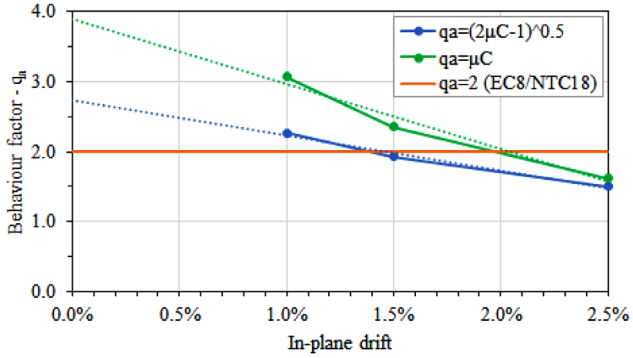

FIGURE 18 Estimation of the behaviour factor q_a for the considered infills

A first rough estimation of the behaviour factor q_a has been here determined starting from the experimental test results, assuming q_a as the ductility capacity μ_C, according to the 'equal displacement rule', or equal to $(2\mu_C - 1)^{0.5}$, according to the 'equal energy rule'. The values of q_a thus calculated are reported in Figure 18, with reference to the values of μ_C reported in Table 3 for TA1, TA2 and TA3. Linear interpolation of such values up to zero drift (dotted lines) is also represented in the figure. This method provides reasonable results when the ratio between the frequency of the panel and that of the seismic action is not particularly large.

As it is possible to notice, the values of q_a decrease as the imposed in-plane drifts increase, which is justifiable from the reduction of the out-of-plane deformation capacity of the panels at larger imposed drifts and therefore at higher damage levels. These values of q_a are found to be higher than the one indicated by EC8[21] and NTC18, MIT,[39] for out-of-plane verifications of masonry infills ($q_a = 2$), at least up to drift values of about 1.50%–2.00%, which are anyhow in line with the ultimate in-plane drift capacity of the tested infill and with the maximum expected deformation demand.

6 | CONCLUSIONS

Within the scope of this study, the effects of combined in-plane and out-of-plane seismic actions on the response of strong clay masonry infills have been investigated based on an extensive, previously accomplished experimental testing campaign, and implications for the infill design and assessment have been derived as a result. A traditional strong clay masonry infill typology, constructed using 35 cm thick tongue and groove clay masonry blocks frequently used for building enclosures in European seismic regions, has been considered.

The results of cyclic and monotonic static out-of-plane tests for fully infilled typologies, both undamaged and previously damaged in-plane, have shown that based on achieved values of out-of-plane strength, for such masonry infill typologies, adherent to the RC frame and without openings, out-of-plane stability is expected to be critical only in regions exposed to high seismicity, since the equivalent accelerations able to activate the maximum out-of-plane force are very large (in this case always larger than about 4 g). Furthermore, a typical bi-directional arching response and related damage patterns could be identified, confirming the formation of a robust resistance mechanism. Therefore, for the specific case of 35 cm thick solid walls tested in this research, it is hard to expect that an earthquake event in the period range of the tested infills may produce such high acceleration demands and cause out-of-plane collapse; however, infills with lower thickness that can be classified as robust (e.g., with perforated blocks characterised by thickness of 20–25 cm), and/or different boundary conditions (e.g., presence of full height openings or defective contacts with the frame) may actually activate the out-of-plane strength with lower levels of seismic action, above all when the in-plane and out-of-plane simultaneous effects are particularly relevant.

Additionally, results of cyclic static test on a previously undamaged masonry stripe, resulting in single-bending conditions have been included for interpretation. Values of out-of-plane strength and stiffness have been related to levels of previous in-plane drift.

Hence, simplified models describing the out-of-plane strength and stiffness reduction for the strong masonry infill have been proposed. Relatively low values of strength degradations are found, above all in comparison with slender/weak masonry typologies. On the contrary, the stiffness has shown a much stronger reduction already from quite low in-plane drifts when the panel starts to be damaged and detached from the frame.

However, for out-of-plane seismic verifications of masonry infills, the normalised resistance reduction coefficient is not per se sufficient but should be always associated to a proper strength criterion for the undamaged infill (i.e., at 0.0% in-plane drift), specifically developed for the considered typology. In this case, an expression based on the vertical arching mechanism theory, duly reduced to take into account flexible supports, out-of-plane deflection and sliding at the infill/structural member interface, has been considered consistent with the experimental results and sufficiently conservative for design/assessment procedures.

In the force-based safety checks, the strength should not be lower than the seismic action force, which depends, among other parameters, on the infill behaviour factor and the elastic period (and therefore, on the elastic stiffness). A simplified expression for the assessment of the period has been proposed, based on the degradation of the stiffness due to cracking and in-plane drift demand. The use of a behaviour factor q_a for infill equal to 2, as requested in the European seismic norms to account in a simplified manner for deformation and energy dissipation capacity, appears to be sufficiently conservative for this strong infill typology, although the approach employed for the derivation of q_a is approximate and further studies are surely needed on this issue.

It is finally important to emphasise that the infill verifications are commonly carried out at ultimate limit state (life safety/severe damage) and that the corresponding in-plane drifts, necessary for the calculation of the infill out-of-plane strength and period, need to be suitably evaluated, eventually applying simplified procedures to obtain the displacement demand of the infilled frame, reducing the displacement demand of the corresponding bare frame.

Due to the limited available data, in particular for the case of strong infills, the proposed reduction models and the expressions for the out-of-plane resistance and stiffness (and period) of the undamaged panel may be further investigated, in order to account more precisely for the related response mechanisms. Moreover, in order to propose specific expressions able to correlate experimental strength and stiffness reduction coefficients coming from different studies as a function of parameters like infill slenderness/thickness, in-plane aspects ratios and boundary conditions, additional tests on some specific infill typologies and a consistent and careful comparison of the experimental results are still needed.

ACKNOWLEDGEMENTS

This work, conducted at the Eucentre Foundation and the Department of Civil Engineering and Architecture of the University of Pavia in Italy, was funded by the ANDIL (Italian Association of Clay Brick and Tile Producers) and by the ReLUIS Projects 2018 and 2019–2021 funded by the Department of the Italian Civil Protection. The financial support received is gratefully acknowledged.

DATA AVAILABILITY STATEMENT

The data that support the findings of this study are available from the corresponding author upon reasonable request.

ORCID

Paolo Morandi https://orcid.org/0000-0002-8999-5491
Riccardo R. Milanesi https://orcid.org/0000-0001-9695-3102
Guido Magenes https://orcid.org/0000-0002-5452-1501

REFERENCES

1. Braga F, Manfredi V, Masi A, Salvatori A, Vona M. Performance of non-structural elements in RC buildings during the L'Aquila, 2009 earthquake. *Bull Earthq Eng*. 2011;9(1):307–324.
2. Ricci P, Manfredi V, De Luca F, Verderame GM. L'Aquila earthquake, Italy: reinforced concrete building performance. *Bull Earthq Eng*. 2011;9:285–305.
3. Manzini CF, Morandi P. Rapporto preliminare sulle prestazioni ed i danneggiamenti agli edifici in muratura portante moderni a seguito degli eventi sismici emiliani del 2012. *Eucentre*. 2012. http://www.eqclearinghouse.org/2012-05-20-italy/
4. Fragomeli A, Galasco A, Graziotti F,et al. Comportamento degli edifici in muratura nella sequenza sismica dell'Italia centrale del 2016 – Parte 1: quadro generale. *Progettazione Sismica*. 2017;8(2):49–77.
5. Vicente R, Rodrigues H, Costa A, Varum H, Mendes da Silva JAR. Performance of masonry enclosure walls: lessons learned from recent earthquakes. *Earthq Eng Eng Vib*. 2012;11(1):23–34.
6. Fardis MN, Bousias SN, Franchioni G, Panagiotakos TB. Seismic response and design of RC structures with plan-eccentric masonry infills. *Earthq Eng Struct Dyn*. 1999;28:173–191.
7. Angel R, Abrams D, Shapiro D, Uzarski J, Webster M. *Behaviour of reinforced concrete frames with masonry infills*, Report-University of Illinois, Urbana-Champaign, Illinois, 1994.
8. Calvi GM, Bolognini D. Seismic response of RC frames infilled with weakly reinforced masonry panels. *J Earthq Eng*. 2001;5(2):153–185.
9. da Porto F, Guidi G, Dalla Benetta M, Verlato N. Combined in-plane/out-of-plane experimental behaviour of reinforced and strengthened infill masonry walls. In: *Proceedings of the 12th Canadian Masonry Symposium*. Vancouver, British Columbia; 2013.
10. Di Domenico M, Ricci P, Verderame GM. Experimental assessment of the influence of boundary conditions on the out-of-plane response unreinforced masonry infill walls. *J Earthq Eng*. 2018:1–39.
11. Furtado A, Rodrigues H, Arede A, Varum H. Experimental evaluation of out-of-plane capacity of masonry infill walls. *Eng Struct*. 2016;111:48–63.
12. Hak S, Morandi P, Magenes G. Out-of-plane experimental response of strong masonry infills. In: *Proceedings of the 2nd ECEES*, Istanbul, Turkey; 2014:25–29.
13. Palieraki V, Zeris C, Vintzileou E, Adami CE. In-plane and out-of-plane response of currently constructed masonry infills. *Eng Struct*. 2018;177:103–116.
14. Ricci P, Di Domenico M, Verderame GM. Experimental investigation of the influence of slenderness ratio and of the in-plane/out-of-plane interaction on the out-of-plane strength of URM infill walls. *Constr Build Mater*. 2018;191:507.
15. Milanesi RR, Morandi P, Magenes G. Out-of-plane response of an innovative masonry infill with sliding joints from shaking table tests. *J Earthq Eng*. 2020. https://doi.org/10.1080/13632469.2020.1739173
16. Manzini CF, Morandi P, Milanesi RR, Magenes G. Shaking-table test on a two-storey RC framed structure with innovative infills with sliding joints. In: *Proceedings of the 16th ECEE*; June 18—21, 2018; Thessaloniki, Greece.
17. Butenweg C, Marinkovic M, Salatic R. Experimental results of reinforced concrete frames with masonry infills under combined quasi-static in-plane and out-of-plane seismic loading. *Bull Earthq Eng*. 2019;17:3397–3422.
18. Di Trapani F, Shing PB, Cavaleri L. Macroelement model for in-plane and out-of-plane responses of masonry infills in frame structures. *J Struct Eng*. 2018;144(2):04017198.
19. Anic F, Penava D, Abrahamczyk L, Sarhosis V. A review of experimental and analytical studies on the out-of-plane behaviour of masonry infilled frames. *Bull Earthq Eng*. 2019;18:2191–2246. https://doi.org/10.1007/s10518-019-00771-5
20. Cavaleri L, Zizzo M, Asteris P. Residual out-of-plane capacity of infills damaged by in-plane cyclic loads. *Eng Struct*. 2020;209:109957.
21. CEN. *Eurocode 8* – Design of structures for earthquake resistance, Part 1: General rules, seismic actions and rules for buildings*, EN 1998-1, European Committee for Standardisation*, Brussels, Belgium; 2004a.
22. MIT, 2018. NTC18: Norme tecniche per le costruzioni [in Italian], D.M. 17/01/2018, G.U. n.42 20/02/2018.

23. Morandi P, Hak S, Magenes G. Simplified Out-of-plane resistance verification for slender clay masonry infills in RC frames. In: *Proceedings Of the XV ANIDIS*, Padova, Italy [in Italian], 2013.
24. Verlato N, Guidi G, da Porto F. Experimental testing and numerical modelling of infill masonry walls subjected to in-plane damage. In: *Proceedings of the 9th International Masonry Conference 2014, 7–9 July 2014*, Guimarães, Portugal, 2014.
25. Furtado A, Rodrigues H, Arede A, Varum H. Effect of the panel width support and columns axial load on the infill masonry walls out-of-plane behaviour. *J Earthq Eng*. 2018;24(4):653–681.
26. Akhoundi F, Vasconcelos G, Lourenço P. Experimental out-of-plane behaviour of brick masonry infilled frames. *Int J Archit Herit*. 2018;14(2):221–237.
27. da Porto F, Donà M, Verlato N, Guidi G. Experimental testing and numerical modeling of robust unreinforced and reinforced clay masonry infill walls, with and without openings. *Front Built Environ*. 2020;6:2020.
28. Al-Chaar G. Evaluating strength and stiffness of unreinforced masonry infill structures. Rep. No. ERDC/CERL TR-02-1; U.S. Army Corps of Engineers: Champaign, IL, USA, 2002.
29. Morandi P, Hak S, Magenes G. Performance-based interpretation of in-plane cyclic tests on RC frames with strong masonry infills. *Eng Struct.* 2018a;156:503–521.
30. CEN. Eurocode 1 – *Actions on structures*, Part 1-1: *General actions – Densities, self-weight, imposed loads for buildings*, EN 1991-1-1, European Committee for Standardisation, Brussels, Belgium, 2002.
31. CEN. *Eurocode 2* – Design of concrete structures*, Part 1-1:* General rules and rules for buildings*, EN 1992-1-1, European Committee for Standardisation*, Brussels, Belgium, 2004b.
32. Morandi P, Hak S, Magenes G. Mechanical characterization and force-displacement hysteretic curves from in-plane cyclic tests on strong masonry infills. *Data Brief*. 2018b;16:886–904.
33. Morandi P, Albanesi L, Magenes G. In-plane cyclic response of new URM systems with thin web and shell clay units. *J Earthq Eng*, 25, 1533-1564, 2019. https://doi.org/10.1080/13632469.2019.1586801
34. Hak S, Morandi P, Magenes G. Prediction of inter-storey drifts for regular RC structures with masonry infills based on bare frame modelling. *Bull Earthq Eng*. 2018;16(1):397–425.
35. Milanesi RR, Morandi P, Hak S, Magenes G. Experiment-based out-of-plane resistance of strong masonry infills for codified applications. *Eng Struct*, 242, 112525, 2021. https://doi.org/10.1016/j.engstruct.2021.112525
36. Drysdale RG, Hamid AA, Baker LR. Masonry Structures: Behaviour and Design. *The Masonry Society*; 1999.
37. Petrone C, Magliulo G, Manfredi G. Floor response spectra in RC frame structures designed according to Eurocode 8. *Bull Earthq Eng*. 2016;14:747–767.
38. Sullivan TJ, Welch DP, Calvi GM. Simplified seismic performance assessment and implications for seismic design. *Earthq Eng Eng Vib*. 2014;13(1):95–122.
39. MIT, 2019. Circolare NTC18. Circolare esplicativa alle Norme tecniche per le costruzioni 2018 [in Italian], C.S.LL.PP. Circolare n. 7, 2019.
40. Chopra AK. *Dynamic of Structures. Theory and Application to Earthquake Engineering*. Pearson Education; 1995.
41. FEMA 306. *Evaluation of Earthquake Damaged Concrete and Masonry Wall Buildings – Basic Procedures Manual*. Federal Emergency Management Agency; 1998.

How to cite this article: Morandi P, Hak S Milanesi RR, Magenes G. In-plane/out-of-plane interaction of strong masonry infills: From cyclic tests to out-of-plane verifications. *Earthquake Engng Struct Dyn*. 2022;51:648–672. https://doi.org/10.1002/eqe.3584

APPENDIX A

Evaluation of out-of-plane resistance and stiffness of specimen TA6 to be consistent with the results of TA1 to TA5 obtained on different loading system.

A.1 | Out-of-plane resistance

In order to directly compare the experimental results of the previously undamaged four-sided supported TA6 with the other specimens previously damaged in-plane, the equivalent out-of-plane resistance of TA6 has been calculated as if the specimen would have been subjected to same loading system adopted for TA1, TA2 and TA3 (fully infilled specimens subjected to strip-loading).

Two simplified procedures have been developed. The first is based on an 'energy/external work' approach, where the applied force (pressure) at collapse and the corresponding deformed shape of the infill have been derived by assuming that the total external work needed to bring the wall to collapse with the two different load distributions (strip loading and uniform loading) is the same. This assumption is deemed to be approximately valid by observing that the crack pattern

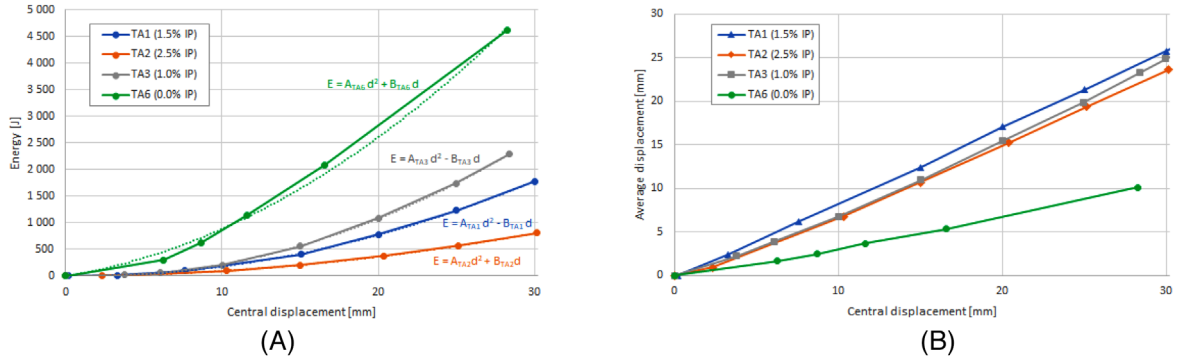

FIGURE A.1 (A) Total energy vs central displacement; (B) 'averaged' displacement of the deformed shape vs central displacement

at out-of-plane collapse for all the specimens tested is similar, suggesting that the total internal work up to collapse is the same for the two loading patterns. The second simplified procedure is based on the equivalence of the moments for the two loading systems assuming the walls behaving in simple vertical bending.

In the 'energy' approach, for each specimen, the cumulative applied energy has been computed incrementally at each step i (E_i) via the volume increments given by displacement increments below the loaded area times the loaded area, and the load (pressure) increments. Such computation was carried out only referring to the monotonic envelope of the force–displacement histories for walls TA1, TA2 and TA3, which were cyclic. Such values of energy are plotted in Figure A.1(A) as a function of the displacement at the centre of the panel. In addition, an effective average displacement d_{ave} value could be associated to each step calculated as the volume V below the loaded area divided by the loaded area A ($d_{ave} = V/A$; $\Delta d_{ave,i} = \Delta V_i/A$).

The values of d_{ave} are reported in Figure A.1(b) as a function of the central displacement at each step of the test (up to the maximum deformation attained in TA6). The displacement d_{ave} is such that the external work done in the test up to displacement $d_{ave,i}$ could be calculated as the integral of the F–d_{ave} curve over the interval $[0; d_{ave,i}]$, where F is the total force applied to the wall. Clearly, since the loaded area for the strip loading is smaller than the total area of the wall, the curve in Figure A.1(B) for wall TA6 (with uniform loading) is different from those of the specimens TA1, TA2, TA3 (strip-loading) which almost overlap on each other.

The plots in Figure A.1(A) provide a different, almost parabolic trend for each specimen, having higher energy for the less damaged (or undamaged) specimens compared to the more damaged ones. To derive the equivalent ultimate load capacity for an undamaged wall with strip loading (i.e., specimen TA6 if it was subjected to a strip loading), the following steps are carried out.

For each central displacement value, the average incremental displacement $\Delta d_{ave,i}$ ($=\Delta V_i/A$) for TA1–TA3 (averaging the three similar plots of Figure A.1(B)) is computed at each ith step of the test.

Moreover, for the same central displacement, a value of ΔE_i is derived from the energy plot of TA6 of Figure A.1(A) and, consequently, also E'_i and δE_i (see Figure A.2) have been computed through the following equations:

$$\Delta E_i = E'_i + \delta E_i \tag{A.1}$$

$$E'_i = F_{i-1} \cdot \Delta V_i/A \tag{A.2}$$

$$\delta E_i = 0.5 \cdot \Delta F_i \cdot \Delta V_i/A \tag{A.3}$$

where ΔE_i is the total energy at the ith step of displacement increment, E'_i is the 'energy/external work' at ith step due to the already existing force computed at the previous step, and δE_i is the 'energy/external work' at the ith step due the increment of force ΔF_i.

The values of ΔF_i are thus computed as:

$$\Delta F_i = \frac{\Delta E_i - E'_i}{0.5 \cdot \frac{\Delta V_i}{A}} = \frac{\delta E_i}{0.5 \cdot \frac{\Delta V_i}{A}} \tag{A.4}$$

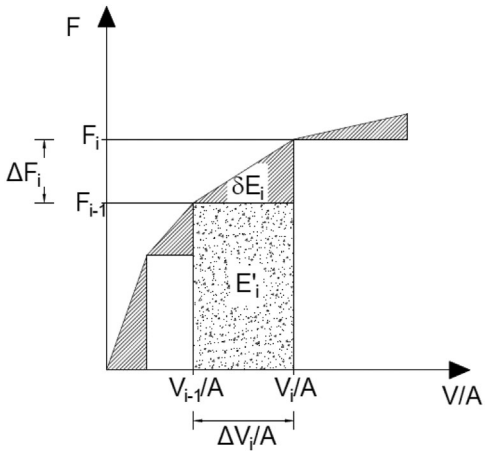

FIGURE A.2 Sketch of the incremental 'energy' method

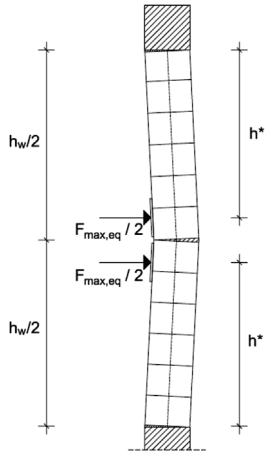

FIGURE A.3 Application of the loads in vertical bending

The summation of ΔF_i at each step up to the maximum displacement attained in the test on TA6 allows to derive the maximum equivalent force of TA6, which has been found to be equal to 274 kN.

The 'energy' method here proposed has been defined specifically for application to this experimental campaign and its application to other setups, loading protocols and specimens is not warranted to provide reliable results in general. Moreover, the goal of the procedure was to estimate the maximum equivalent force for the strip-loading case at collapse (i.e., the last point of the force displacement curve, but not the previous ones), where a complete activation of the cracking/crushing mechanism and the resulting two-way arching mechanism has completely developed. Other applications of this method could possibly be thought with further developments, trying also to reduce its numerical sensitivity, although for the present application the results obtained seem in line with those obtained with the other approximated approach, which is described as follows.

The second approach for the evaluation of the equivalent force of TA6 takes into account vertical bending only, through the equivalence of the moments between the loading system of TA6 and the linear loading pattern of TA1 to TA3.

$$M_R = \frac{w_{\max}^{TA6} \cdot h_w^2 \cdot L_w}{8} = \frac{F_{\max,eq} \cdot h^*}{2} \tag{A.5}$$

where $w_{\max}{}^{TA6}$ is the maximum experimental pressure attained by TA6, h_w and L_w are the height and the length of the infill, h^* is the distance between the top/bottom end section of the infill to the point of application of the linear loads of TA1 to TA3 ($h^* = 1.30$ m), $F_{\max,eq}$ is the equivalent force requested (see Figure A.3). According to Equation A.5, the maximum equivalent force $F_{\max,eq}$ is 256 kN.

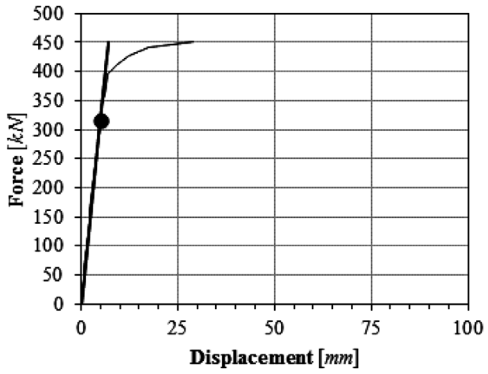

FIGURE A.4 Force–displacement response of TA6 with the indication of the elastic secant stiffness

The two methods provide rather similar results, demonstrating the validity of the assumptions used in the 'energy' approach, whose evaluated resistance has been adopted in the findings of this article.

A.2 | Out-of-plane elastic stiffness

The out-of-plane elastic stiffness of TA6 has been computed as the ratio between a force of $0.7F_{max}$ and the corresponding displacement ($k_{el} = 315/5.04 = 62.5$ kN/mm) as reported in Figure A.4.

Then, a linear elastic FEM analysis of the infill has been carried out; the panel has been modelled through shell elements simply supported on the four edges made of an orthotropic material using the elastic moduli of the vertical and horizontal direction derived by the tests of characterisation ($E_{mv} = 5299$ MPa, $E_{mh} = 494$ MPa, $G = 0.05E_{mv} = 265$ MPa) and applying a distributed load as in the test of TA6 at 0.7 F_{max} (=0.70·36.2 = 25.3 kN/m^2). In order to match the experimental deflections at 0.7 F_{max} (=5.04 mm), a value of the cracking coefficient $\alpha_{cr} = 0.27$, reducing the uncracked flexural and shear stiffness of masonry, was found.

Finally, such a calibrated model has been loaded with the same loading system of TA1 to TA3 until the central displacement was the same of the one of TA6 at 0.7 F_{max}. The value of the total force thus found, divided by the central displacement, was estimated to be the equivalent stiffness of TA6* (TA6 with the loading system of TA1 to TA3), $k_{el} = 27.0$ kN/mm.